Floquet topological systems in the vicinity of band crossings: Reservoir-induced coherence and steady-state entropy production

Hossein Dehghani and Aditi Mitra
Department of Physics, New York University, 4 Washington Place, New York, New York 10003, USA
(Received 1 December 2015; revised manuscript received 31 May 2016; published 16 June 2016)

Results are presented for an open Floquet topological system represented by Dirac fermions coupled to a circularly polarized laser and an external reservoir. It is shown that when the separation between quasienergy bands becomes small, and comparable to the coupling strength to the reservoir, the reduced density matrix in the Floquet basis, even at steady state, has nonzero off-diagonal elements, with the magnitude of the off-diagonal elements increasing with the strength of the coupling to the reservoir. In contrast, the coupling to the reservoir only weakly affects the diagonal elements, hence inducing an effective coherence. The steady-state reduced density matrix synchronizes with the periodic drive, and a Fourier analysis allows the extraction of the occupation probabilities of the Floquet quasienergy levels. The lack of detailed balance at steady state is quantified in terms of an entropy-production rate, and it is shown that this equals the heat current flowing out of the system and into the reservoir. It is also shown that the entropy-production rate mainly depends on the off-diagonal components of the Floquet density matrix. Thus, a stronger coupling to the reservoir leads to an enhanced entropy-production rate, implying a more efficient removal of heat from the system, which in turn helps the system maintain coherence. Analytic expressions in the vicinity of the Dirac point are derived which highlights these results, and also indicates how the reservoir may be engineered to enhance the coherence of the system.

DOI: 10.1103/PhysRevB.93.245416

I. INTRODUCTION

The study of periodically driven systems has seen a resurgence in recent years, appearing in many different contexts such as periodic drive as a means for realizing myriad topological phases [1–10], as non-energy-conserving examples of systems exhibiting many-body localization [11–14], and as examples of systems that can support novel collective behavior absent in static Hamiltonians [15,16]. While plenty of physical insight can be gained by mapping the time-dependent Hamiltonian into an effective time-independent Hamiltonian (the Floquet Hamiltonian) that captures the time evolution over one period [17], ultimately it is the distribution function of the particles that needs to be properly accounted for in order to understand how much of the physics extracted simply from a spectral analysis of the Floquet Hamiltonian survives.

The distribution function depends on the dominant relaxation mechanisms, i.e., whether it is a good approximation to think of the periodically driven system to be isolated from its surroundings so that the drive switch on protocol or the interactions between particles determine the distribution function [18–26]. In contrast, it could also be that the the system is coupled to external leads, but is short in comparison to electron-electron or electron-phonon (el-ph) scattering lengths, so that it is the leads that impose the occupation probabilities [27–30]. Finally, another commonly encountered example is inelastic relaxation due to the system being coupled to an external reservoir [21,22,31–33]. In this paper, we consider the last case discussed above, namely, a periodically driven open system, where the inelastic scattering with a reservoir determines the distribution function. We will be interested in a circularly polarized drive which when applied to graphene, opens up a topologically nontrivial gap at the Dirac points, inducing a Chern insulator [1,10]. Our work here differs from our previous work on a similar system [20–22] in that we in this work specifically consider the case where one is close to a topological phase transition, so that the separation between quasienergy bands is comparable to the coupling to an external reservoir. Our past work was in the opposite limit where the quasienergy level spacings were large as compared to coupling to an external reservoir, and thus we were far from any topological phase transitions.

One of the main new results in this regime is that we find an effective reservoir-induced coherence where the steady state involves nonzero off-diagonal elements of the Floquet density matrix that grow with the strength of the coupling to the reservoir, while the diagonal elements are relatively weakly affected. This leads to an effective reduced density matrix $W_{\rm el}$ which becomes purer, i.e., $\mathrm{Tr}[(W_{\rm el})^2]$ increases with the coupling to the reservoir.

Another new ingredient in this work is that, while it is known that generic driven dissipative systems reach steady states that cannot be described by an effective temperature, and hence do not resemble a Gibbs distribution [20,34–36], in this work we characterize this lack of detailed balance by a net steady-state entropy-production rate. We prove that in the steady state where the density matrix has synchronized with the external drive, the entropy production mainly depends on the off-diagonal components of the density matrix. Thus, the more coherent the system becomes, the larger is the entropy-production rate. This is not paradoxical because the steady-state entropy-production rate equals the heat current flowing out of the system and into the reservoir. Thus, the more efficient this flow is, the more effective the system is in maintaining coherence.

We obtain analytic expressions in the vicinity of the Dirac point, and use this to highlight the above general observations. Our results also indicate how a reservoir can be engineered to control the entropy-production rate. In fact, enhancing the latter can cause the system to settle into more coherent and possibly even dark states where $\mathrm{Tr}[(W_{\rm el})^2] = 1$.

The paper is organized as follows. In Sec. II, we describe the model and outline the derivation of the Floquet master equation, highlighting the approximations that fail once quasienergy level spacings become small. In Sec. III, we discuss our results for the reduced density matrix and extract the occupation probabilities of the Floquet quasienergy levels, while in Sec. IV we quantify the lack of detailed balance in terms of a steady-state entropy-production rate. Finally, we conclude in Sec. V. Some details are relegated to the Appendices. Appendix A shows that all the components of the steady-state density matrix are synchronized with the laser frequency. Appendix B derives a general relation between the entropy-production rate and the steady-state density matrix, and shows by means of an analytic calculation at the Dirac point, that the entropy-production rate is mainly controlled by the off-diagonal components of the density matrix. Appendix C provides details needed for arriving at the analytic expressions at the Dirac point.

II. MODEL

In the vicinity of a laser-induced topological phase transition in graphene, we may approximate graphene as Dirac fermions under a periodic drive. This model can also alternately describe a laser applied to the two-dimensional (2D) surface states of a three-dimensional (3D) topological insulator (TI) [37]. The Hamiltonian of 2D Dirac fermions coupled to an external circularly polarized laser, and also coupled to a reservoir of phonons, is

$$H = H_{\rm el} + H_{\rm ph} + H_c, \tag{1}$$

where (setting $\hbar = 1$)

$$H_{\rm el} = \sum_{\vec{k}=[k_x,k_y],\sigma,\sigma'=\uparrow,\downarrow} c^\dagger_{\vec{k}\sigma}[\vec{k} + \vec{A}(t)]\cdot\vec{\sigma}_{\sigma\sigma'}c_{\vec{k}\sigma'}. \tag{2}$$

$c^\dagger_{\vec{k}\sigma}, c_{\vec{k}\sigma}$ are creation, annihilation operators for the Dirac fermions whose velocity $v = 1$, $\vec{\sigma} = [\sigma_x,\sigma_y]$ are the Pauli matrices which represent spins of surface states of a 3D TI, or it represents the sublattice label for graphene. $\vec{A} = \theta(t)A_0[\cos(\Omega t), -\sin(\Omega t)]$ is the circularly polarized laser which has been suddenly switched on at time $t = 0$, we will refer to this switch-on protocol as a quench. We will denote the period of the laser as $T_\Omega = 2\pi/\Omega$ and the temperature of the reservoir as T.

Here, we consider coupling to 2D phonons

$$H_{\rm ph} = \sum_{q,i=x,y}[\omega_{qi}b^\dagger_{qi}b_{qi}], \tag{3}$$

where the electron-phonon coupling is

$$H_c = \sum_{\vec{k},q,\sigma,\sigma'} c^\dagger_{\vec{k}\sigma}\vec{M}_{\rm ph}(k,q)\cdot\vec{\sigma}_{\sigma\sigma'}c_{\vec{k}+\vec{q}\sigma'}, \tag{4}$$

$$\vec{M}_{\rm ph}(k,q) = [\lambda_{x,kq}(b^\dagger_{x,q} + b_{x,-q}),\lambda_{y,kq}(b^\dagger_{y,q} + b_{y,-q})]. \tag{5}$$

There is no σ_z term above because we have adopted a model for electron-phonon coupling consistent for graphene [38], where the electron-phonon coupling should preserve A-B sublattice symmetry. Such a symmetry is broken by terms proportional to σ_z.

In the absence of electron-phonon coupling, the problem is exactly solvable, where the time evolution from time t_0 to t is

$$|\Psi(t)\rangle = U_{\rm el}(t,t_0)|\Psi(t_0)\rangle. \tag{6}$$

For a spatially invariant system, the time-evolution operator factorizes into different momenta k, $U_{\rm el}(t,t') = \prod_k U_{{\rm el},k}(t,t')$, with

$$U_{{\rm el},k}(t,t') = \sum_{\alpha=u,d} e^{-i\epsilon_{k\alpha}(t-t')}|\phi_{k,\alpha}(t)\rangle\langle\phi_{k\alpha}(t')|, \tag{7}$$

where $\epsilon_{k\alpha}$ are the quasienergies and $|\phi_{k\alpha}(t)\rangle$ are the time-periodic quasimodes. The quasimodes and quasienergies satisfy the following eigenvalue equation:

$$H^F_{\rm el}|\phi_{k,\alpha}\rangle = \epsilon_{k\alpha}|\phi_{k,\alpha}\rangle, \tag{8}$$

where $H^F_{\rm el} \equiv H_{\rm el}(t) - i\partial_t$ is known as the Floquet Hamiltonian. Note that it is the combination $|\psi_{k\alpha}\rangle \equiv e^{-i\epsilon_{k\alpha}t}|\phi_{k\alpha}(t)\rangle$ that obeys the time-dependent Schrödinger equation for $H_{\rm el}(t)$, and since we are considering a two-level Hamiltonian at every momentum k, there are only two distinct solutions that we label as $\alpha = u,d$.

Once the system is coupled to phonons, the problem is not exactly solvable, and in fact on integrating out the phonon modes, it is straightforward to see that we have an interacting electron problem. We make progress by making certain assumptions: that the coupling to the phonons is weak, only interband transitions between the quasienergy levels are allowed [i.e, $\vec{M}_{\rm ph}(k,q)$ is peaked at $q = 0$], and that the phonons are always in thermal equilibrium at the temperature T.

Our assumption for neglecting intraband transitions is based on the fact that these occur on longer time scales than interband transitions. This is because the energy exchange for the former is smaller than the latter, and also because typical electron-phonon matrix elements are stronger for optical phonons compared with acoustic phonons [39]. Thus, there is an intermediate time scale where the results obtained purely from inter-band transitions will be valid. In the next section, we outline the derivation of the Floquet master equation based on these assumptions.

A. Rate equation

Let $W(t)$ be the density matrix in the Schrödinger picture, obeying

$$\frac{dW(t)}{dt} = -i[H,W(t)]. \tag{9}$$

To obtain the rate equation, it is convenient to be in the interaction representation $W^I(t) = e^{iH_{\rm ph}t}U^\dagger_{\rm el}(t,0)W(t)U_{\rm el}(t,0)e^{-iH_{\rm ph}t}$. To $\mathcal{O}(H_c^2)$, the density matrix obeys the following equation of motion:

$$\frac{dW^I}{dt} = -i\big[H^I_c(t),W^I(t_0)\big] - \int_{t_0}^t dt'\big[H^I_c(t),\big[H^I_c(t'),W^I(t')\big]\big], \tag{10}$$

where H^I_c is in the interaction representation. We assume that at the initial time t_0, the electrons and phonons are uncoupled

so that $W(t_0) = W_{\mathrm{el},0}(t_0) \otimes W_{\mathrm{ph}}(t_0)$. We assume that initially, before the laser has been switched on, the electrons are in the ground state of Dirac fermions, while the phonons are in thermal equilibrium at temperature T.

Thus, for a laser quench at $t = 0$,

$$W^0_{\mathrm{el}}(t) = |\Psi(t)\rangle\langle\Psi(t)| = \prod_k W^0_{\mathrm{el,k}}, \tag{11}$$

where

$$W^0_{\mathrm{el,k}}(t) = \sum_{\alpha,\beta=\pm} e^{-i(\epsilon_{k\alpha}-\epsilon_{k\beta})t}|\phi_{k\alpha}(t)\rangle\langle\phi_{k\beta}(t)|\rho^{I,\mathrm{quench}}_{k,\alpha\beta} \tag{12}$$

with

$$\rho^{I,\mathrm{quench}}_{k,\alpha\beta} = \langle\phi_{k\alpha}(0)|\psi_{\mathrm{in},k}\rangle\langle\psi_{\mathrm{in},k}|\phi_{k\beta}(0)\rangle, \tag{13}$$

$$|\psi_{\mathrm{in},k}\rangle = \frac{1}{\sqrt{2}}\begin{pmatrix} -(k_x - ik_y)/k \\ 1 \end{pmatrix}. \tag{14}$$

The above is simply stating that for a quench, the occupation of the Floquet levels ($\rho^{I,\mathrm{quench}}_{k,\alpha\beta}$) is simply given by their overlap with the ground state $|\psi_{\mathrm{in},k}\rangle$ of the Dirac fermions.

Defining the electron reduced density matrix as the one obtained from tracing over the phonons, $W_{\mathrm{el}} = \mathrm{Tr}_{\mathrm{ph}} W$, and noting that H_c being linear in the phonon operators, the trace vanishes, we need to solve

$$\frac{dW^I_{\mathrm{el}}}{dt} = -\mathrm{Tr}_{\mathrm{ph}}\int_{t_0}^{t} dt'\big[H^I_c(t),\big[H^I_c(t'),W^I(t')\big]\big]. \tag{15}$$

We assume that the phonons are an ideal reservoir and stay in equilibrium with temperature T. In that case, $W^I(t) = W^I_{\mathrm{el}}(t) \otimes e^{-H_{\mathrm{ph}}/T}/\mathrm{Tr}[e^{-H_{\mathrm{ph}}/T}]$ (we set $k_B = 1$).

The most general form of the reduced density matrix for the electrons is

$$W^I_{\mathrm{el}}(t) = \prod_k \sum_{\alpha\beta} \rho^I_{k,\alpha\beta}(t)|\phi_{k,\alpha}(t)\rangle\langle\phi_{k,\beta}(t)|, \tag{16}$$

where in the absence of phonons, $\rho^I_{k,\alpha\beta} = \rho^{I,\mathrm{quench}}_{k,\alpha\beta}$ and are time independent in the interaction representation. With phonons, $\rho^I_{k,\alpha\beta}(t)$ are time dependent. We make the Markov assumption that the reservoir correlation times are very fast as compared to the time scale over which ρ^I_k vary [34,35]. This allows us to pull the $\rho(t')$ out of the integral above, leading to the Floquet master equation. Since eventually one is interested in the density matrix in the Schrödinger representation, here we present the Floquet master equation in the Schrödinger picture. Before doing this, let us define our notation for the density matrix in the Schrödinger picture

$$W_{\mathrm{el}}(t) = \prod_k \sum_{\alpha\beta} \rho^S_{k,\alpha\beta}(t)|\phi_{k,\alpha}(t)\rangle\langle\phi_{k,\beta}(t)|, \tag{17}$$

where $\rho^S_{k,\alpha\beta} = \rho^I_{k,\alpha\beta}e^{-i(\epsilon_{k\alpha}-\epsilon_{k\beta})t}$. Since in all of our future results we use $\rho^S_{k,\alpha\beta}$, we will drop the superscript S after this. Using this notation, the Floquet master equation becomes

$$\begin{aligned}\dot{\rho}_{k,\alpha\beta}(t) &+ i(\epsilon_{k\alpha} - \epsilon_{k\beta})\rho_{k,\alpha\beta}(t) \\ &= -\sum_{\delta\gamma}\big[R^k_{\alpha\delta,\delta\gamma}(t)\rho_{k,\gamma\beta}(t) + \rho_{k,\alpha\gamma}(t)R^{k*}_{\beta\delta,\delta\gamma}(t) \\ &\quad -\rho_{k,\delta\gamma}(t)R^{k*}_{\delta\alpha,\beta\gamma}(t) - \rho_{k,\gamma\delta}(t)R^k_{\delta\beta,\alpha\gamma}(t)\big],\end{aligned} \tag{18}$$

where R is the transition or rate matrix. Assuming a uniform phonon density of states ν and denoting N as the Bose distribution function at temperature T, we can use the fact that the rate matrix R has the periodicity of the laser to Fourier expand it:

$$R^k_{\alpha\beta,\alpha'\beta'}(t) = \sum_{n_1,n_2} e^{i(n_2-n_1)\Omega t}R^{n_2,n_1}_{\alpha\beta,\alpha'\beta'}, \tag{19}$$

$$\begin{aligned}R^{n_2,n_1}_{\alpha\beta,\alpha'\beta'} &= [(1 + N[\epsilon_{k\beta'} - \epsilon_{k\alpha'} + n_1\Omega])\theta(\epsilon_{k\beta'} - \epsilon_{k\alpha'} + n_1\Omega) \\ &\quad + N[-\epsilon_{k\beta'} + \epsilon_{k\alpha'} - n_1\Omega]\theta(-\epsilon_{k\beta'} + \epsilon_{k\alpha'} - n_1\Omega)] \\ &\quad \times\big[\big(C^{n_2}_{1\alpha\beta}C^{-n_1}_{1\alpha'\beta'} + C^{n_2}_{2\alpha\beta}C^{-n_1}_{2\alpha'\beta'}\big)\nu\big(\lambda_x^2 - \lambda_y^2\big) \\ &\quad + \big(C^{n_2}_{1\alpha\beta}C^{-n_1}_{2\alpha'\beta'} + C^{n_2}_{2\alpha\beta}C^{-n_1}_{1\alpha'\beta'}\big)\nu\big(\lambda_x^2 + \lambda_y^2\big)\big],\end{aligned} \tag{20}$$

where $C^n_{1,2}$ are the Fourier transform of the following matrix elements:

$$\langle\phi_{k\alpha}(t)|c^\dagger_{k\uparrow}c_{k\downarrow}|\phi_{k\beta}(t)\rangle = \sum_n e^{in\Omega t}C^n_{1k\alpha\beta}, \tag{21}$$

$$\langle\phi_{k\alpha}(t)|c^\dagger_{k\downarrow}c_{k\uparrow}|\phi_{k\beta}(t)\rangle = \sum_n e^{in\Omega t}C^n_{2k\alpha\beta}. \tag{22}$$

Due to our choice of the electron-phonon coupling, any phonon absorption and emission takes place via spin/pseudospin flips as can be seen explicitly from the structure of the matrix elements $C_{1,2}$. It is also useful to note that under complex conjugation we have

$$R^{k*}_{\alpha\beta,\alpha'\beta'}(t) = \sum_{n_1,n_2} e^{i(n_2-n_1)\Omega t}\big[R^{-n_2,-n_1}_{\alpha\beta,\alpha'\beta'}\big]^*. \tag{23}$$

From Eq. (20), it is clear that $R^{n_2,n_1}_{\alpha\beta,\alpha'\beta'}$ is the Fermi golden rule rate for making a transition from quasienergy level $\epsilon_{k\alpha'}$ to $\epsilon_{k\beta'} + n_1\Omega$ by phonon absorption or emission. Since $\alpha,\beta = u,d$, we see that this rate includes processes that change the electronic state ($\alpha \neq \beta$) as well as Floquet-umpklapp processes where the electron state remains the same $\alpha = \beta$, but the system absorbs or emits phonons at energy $n_1\Omega$. As we shall later discuss, the latter processes are particularly important for achieving reservoir-induced coherence as they take away the energy being supplied by the periodic drive without changing the electronic state (since $\alpha = \beta$).

If we had relaxed the assumption that the phonons were in equilibrium at temperature T, then the functions $N(\epsilon) = \langle b^\dagger_\epsilon b_\epsilon\rangle, 1 + N(\epsilon) = \langle b_\epsilon b^\dagger_\epsilon\rangle$ entering the rates would have been unknown, and a separate kinetic equation would have to be written for them, leading to a complex electron-phonon coupled Boltzmann equation.

We now mention some additional commonly made assumptions to further simplify the rate equation (18). When the separation between quasienergy levels is large as compared to the coupling to the reservoir, the off-diagonal matrix elements of the density matrix in the Floquet basis become small, and can be neglected [35]. In this case, the steady-state solution for the density matrix, even though it bears little resemblance to a Gibbs distribution (unless of course the frequency of the laser is large as compared to the electron bandwidth), is independent of the electron-reservoir coupling [20,21]. The simplest way to see this lack of dependence on the coupling is to notice that when the off-diagonal elements of the density matrix are zero in Eq. (18), the diagonal elements at steady state are

given by the ratio of some combination of the rates R. Since each R depends on the electron-phonon coupling by being proportional to $\nu\lambda^2_{x,y}$, the coupling dependence falls off in the steady-state result for the density matrix when $\lambda_x = \lambda_y$. When $\lambda_x \neq \lambda_y$, the result depends on the coupling only via the asymmetry ratio λ_x^2/λ_y^2. The resulting distribution at steady state is isotropic in momentum space when $\lambda_x = \lambda_y$, while it can be anisotropic in momentum space for $\lambda_x \neq \lambda_y$.

In addition, if the coupling to the reservoir is small in comparison to the drive frequency Ω, then the steady-state density matrix varies slowly over one cycle of the drive. In this case, one may make the "modified rotating wave approximation" [34,35] which involves replacing the scattering rates $R(t)$ by their average over one cycle. We call this case the time-averaged Floquet master equation. In what follows, we will not make either of the above assumptions, i.e., we will retain the off-diagonal component of the density matrix and keep the full time dependence of $R(t)$, i.e, we will solve Eq. (18) directly.

In the remaining paper, we present all results for isotropic electron-phonon couplings ($\lambda_x = \lambda_y = \lambda$). Since the resulting distribution is isotropic in momentum space, we will present results along $k_y = 0$. We also set the phonon density of states to be uniform and equal to $\nu = 1$. Thus, we assume that we have nonzero phonon density of states at all relevant energy scales. We supplement these results with analytic results at $k = 0$ that highlight how the energy dependence of the phonon density of states affects the steady state.

We present our numerical results for phonon temperature $T = 0.1\Omega$ and three different reservoir coupling strengths $\lambda/\Omega = 0.08, 0.16, 0.2$ and in those cases where the results are weakly dependent on λ, we only present the results for $\lambda/\Omega = 0.08, 0.2$. We also fix the laser amplitude to $A_0/\Omega = 0.5$. The corresponding quasienergy spectra plotted within the first Floquet Brillouin zone (FBZ) ($|\omega| < \Omega/2$) is shown in Fig. 1, showing the topological gap opening at $k = 0$. This curve can be compared with the dashed line in this plot which illustrates an ideal repeated Dirac band structure in the Floquet zone. For weak laser frequencies ($A_0/\Omega \ll 1$), we

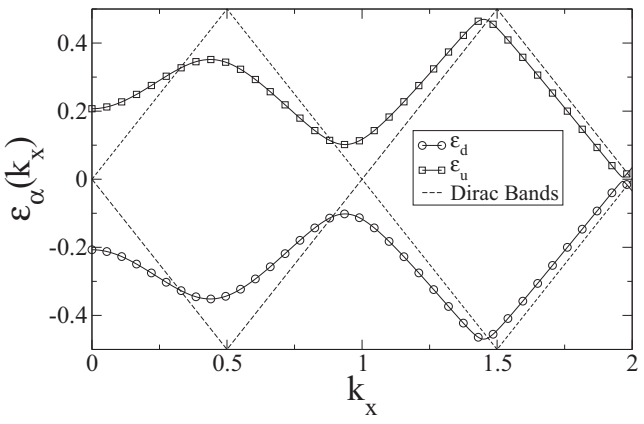

FIG. 1. Quasienergy spectrum in the first FBZ for $A_0/\Omega = 0.5$ along $k_y = 0$, and compared with the Dirac spectrum in the absence of the laser. We have set $\Omega = 1.0$. The gap at $k = 0$ is topological and equals $\epsilon_u - \epsilon_d = (\sqrt{4A_0^2 + \Omega^2} - \Omega)$.

expect resonances at $|k| \sim n\Omega/2$, with this condition shifting as the laser amplitude increases. The resonances are reflected by the narrowing of the quasienergy level spacings at these k points and, in what follows, special attention will be given to the occupation probabilities in the vicinity of these points, showing that the off-diagonal components of the density matrix also become larger here.

The master equation (18) is a linear ordinary differential equation (ODE) of order one with time-dependent coefficients. From ODE theory we know that such differential equations have closed solutions. While our results are based on numerical simulations of these equations, and an analytic solution at $k = 0$, there are some general features in the steady state of these solutions which we discuss in Appendix A. In particular, one can show that in the steady state which is reached after an initial transient whose duration is controlled by $\lambda^2\nu$, the density matrix synchronizes with the laser field. Thus, the only oscillations remaining in the system are those with frequency Ω and its multiples. This can at first seem counterintuitive especially for off-diagonal components of the density matrix because one may naively expect from the term $i(\epsilon_{k\alpha} - \epsilon_{k\beta})\rho_{k,\alpha\beta}$ on the left-hand side of the master equation (18) that the off-diagonal components must oscillate with the frequency $(\epsilon_{k\alpha} - \epsilon_{k\beta})$. As explained in Appendix A, while this is valid initially, in the steady state these oscillations decay due to the presence of the electron-phonon coupling terms on the right-hand side of the master equation. Therefore, in the steady state we can expand the density matrix via a Fourier series

$$\rho^{\rm SS}_{k,\alpha\beta}(t) = \sum_m e^{im\Omega t}\rho^m_{k,\alpha\beta}, \tag{24}$$

where the superscript SS denotes the steady state. Above one may interpret $|\rho^m_{k,\alpha\alpha}|$ as the occupation of the mth Floquet state of quasienergy $\epsilon_{k\alpha} - m\Omega$, and $|\rho^m_{k,\alpha\beta}|$ is the probability of being in a coherent superposition of the quasienergy levels $\epsilon_{k\beta}$ and $\epsilon_{k\alpha} - m\Omega$. Furthermore, as we show later, the entropy-production rate depends on $\partial_t\rho^{\rm SS}_{k,\alpha\beta}$. Thus, the Fourier expansion coefficients $|\rho^m_{k,\alpha\beta}|$ find physical significance in terms of the entropy produced and heat released to the environment. In what follows, we will give explicit results for the parameters mentioned above.

III. RESULTS FOR THE REDUCED DENSITY MATRIX

Figure 2 shows how the diagonal and off-diagonal components of the reduced density matrix evolve in time for two different electron-phonon coupling strengths and for a particular momentum, we have chosen $k_x = 0.3$, $k_y = 0$. Quite generically, the steady state is periodic with frequency Ω, and the larger the electron-phonon coupling λ, the larger is the magnitude of oscillations in the steady state. These oscillations originate from the the nonzero Fourier harmonics of the R matrix. In fact, as we show in Appendix A, in a Floquet master equation with a time averaged R, the steady-state oscillations of $\rho_{k,\alpha\beta}$ disappear.

The time-averaged value of the reduced density matrix is such that the diagonal component is not very sensitive to λ as can be seen in Fig. 3. In this figure, in addition to the populations in the presence of the electron-phonon coupling, there

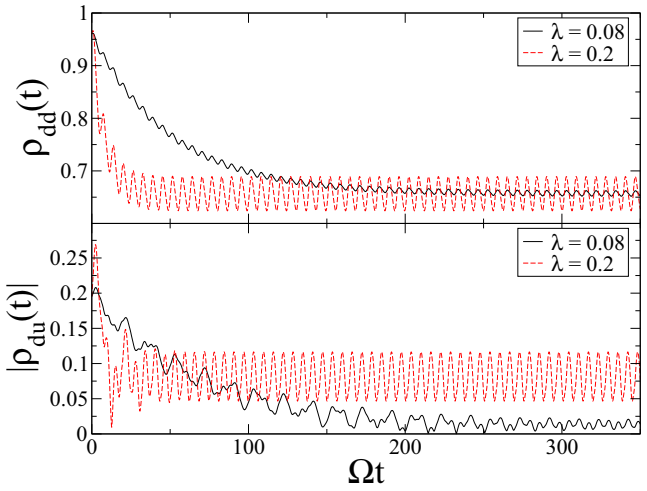

FIG. 2. Time evolution of the diagonal (upper-panel) and off-diagonal (lower-panel) components of the reduced density matrix at momentum $k_x = 0.3$, $k_y = 0$, for electron-phonon coupling strengths of $\lambda/\Omega = 0.08, 0.2$, and phonons at temperature $T = 0.1\Omega$. We have set $\Omega = 1.0$. Increasing λ/Ω decreases the time to reach steady state, increases the amplitude of the steady-state oscillations, and increases the magnitude of the time averaged ρ_{du}, while only weakly affecting the magnitude of the time averaged ρ_{dd}.

is another curve depicting the thermal distribution, denoted by $\rho^{\text{Gibbs}}_{k,dd} = 1 - \rho^{\text{Gibbs}}_{k,uu}$ and given by $\rho^{\text{Gibbs}}_{k,uu} = (1 + e^{(\epsilon_{ku} - \epsilon_{kd})/T})^{-1}$. The figure shows that $\rho^{\text{Gibbs}}_{k,dd}$ is always close to 1, except around the resonances $k \sim \Omega, 2\Omega$ when the quasienergy level separation becomes small. Moreover, the Gibbs distribution and the reservoir-induced distributions can be very different. In Ref. [20], we showed how the reservoir-induced distribution and the Gibbs distribution approach each other at small momenta ($k \ll \Omega$) as A_0/Ω becomes small, i.e., in the highly off-resonant case.

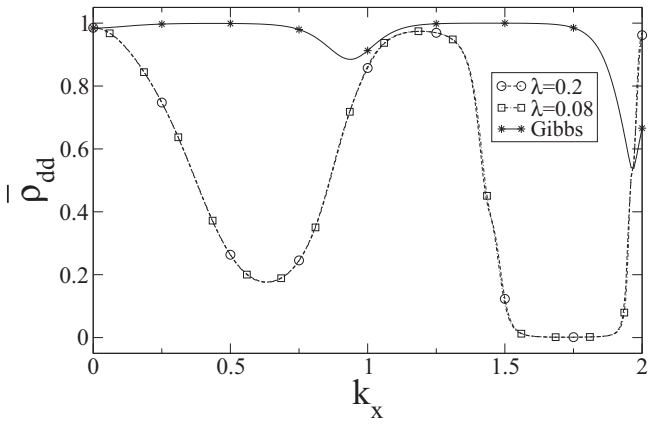

FIG. 3. Time-averaged diagonal component of the density matrix for the "down" Floquet level ($\bar{\rho}_{dd}$) for $\lambda/\Omega = 0.08, 0.2$, and reservoir temperature $T = 0.1\Omega$. This is compared with the Gibbs distribution $\rho^{\text{Gibbs}}_{dd} = e^{(\epsilon_u - \epsilon_d)/T}/(1 + e^{(\epsilon_u - \epsilon_d)/T})$. We have set $\Omega = 1.0$, $k_y = 0$. λ only weakly affects $\bar{\rho}_{dd}$, however, the latter is far from a Gibbs state.

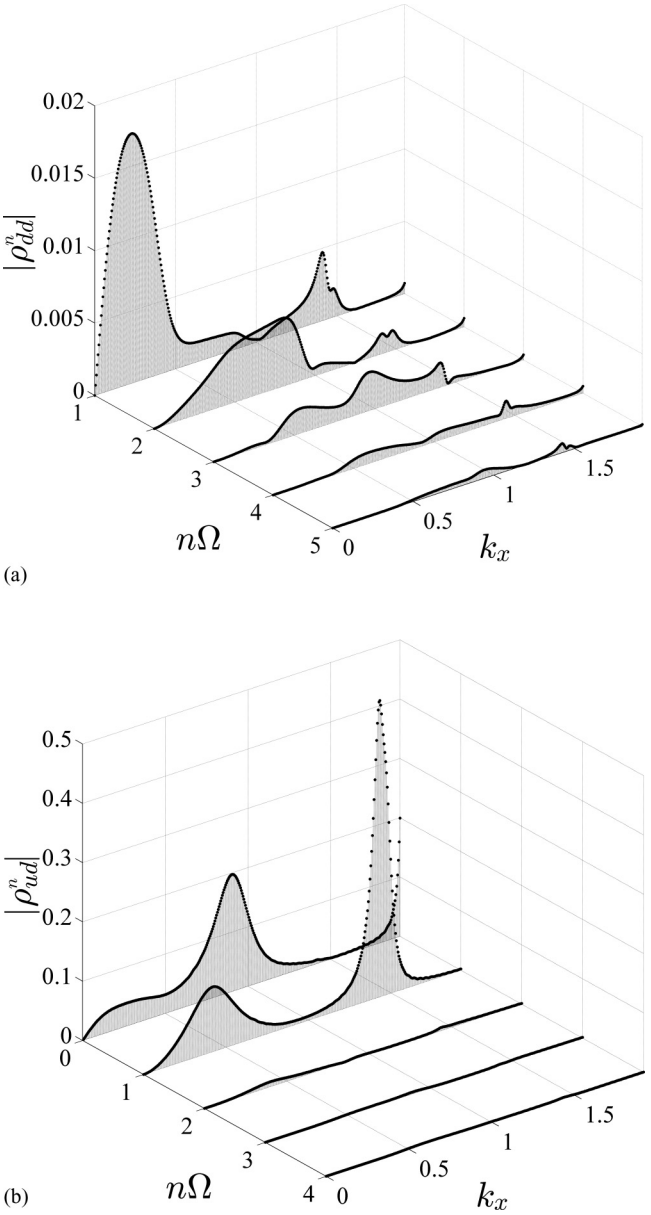

FIG. 4. Fourier transform of the (a) diagonal ρ^n_{dd} and (b) off-diagonal ρ^n_{ud} components of the reduced density matrix at steady state, for $\lambda/\Omega = 0.2$, $k_y = 0$ and reservoir temperature $T = 0.1\Omega$. The $|\rho^n_{dd}|$ are the occupation probability of the $\epsilon_d - n\Omega$ quasienergy level, while $|\rho^n_{ud}|$ the probability of being in a coherent superposition of quasienergy levels ϵ_d and $\epsilon_u - n\Omega$. We have set $\Omega = 1.0$. Note that $\rho^{n=0}_{dd}$ is not shown as it is already plotted in Fig. 3.

Since the steady-state density matrix is periodic in Ω, we can Fourier transform it according to Eq. (24), and the results for $\lambda = 0.2$ are shown in Fig. 4, and those for the smaller coupling of $\lambda = 0.08$ are shown on Fig. 5. We only show positive harmonics, as $|\rho^n_{\alpha\beta}|$ are symmetric under n to $-n$. One finds that as one approaches the resonance condition $k_x \sim \Omega/2, \Omega, 3\Omega/2 \ldots$, higher and higher harmonics of the density matrix are excited, with their magnitude also increasing with the coupling λ to the reservoir. The reservoir dependence in $|\rho^n_{ud}|$ is shown more clearly in Fig. 6 where a direct comparison has been made between three different couplings

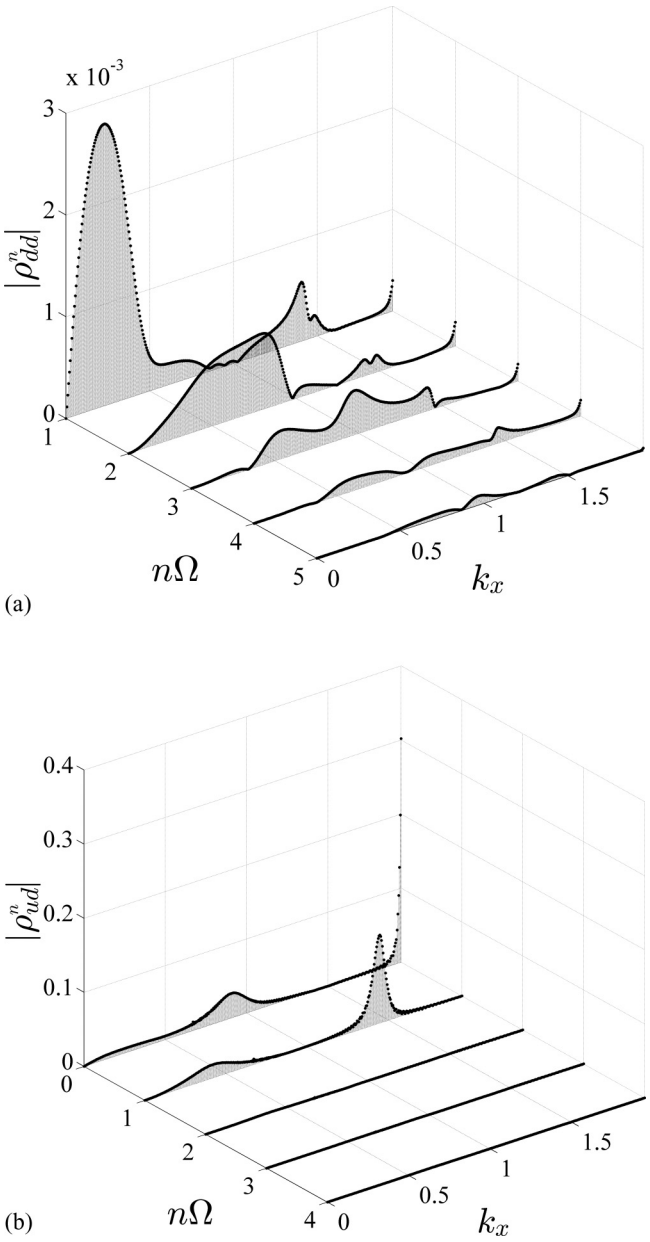

FIG. 5. Fourier transform of the (a) diagonal ρ^n_{dd} and (b) off-diagonal ρ^n_{ud} components of the reduced density matrix at steady state, for $\lambda/\Omega = 0.08$, $k_y = 0$ and reservoir temperature $T = 0.1\Omega$. We have set $\Omega = 1.0$. Note that $\rho^{n=0}_{dd}$ is not shown as it is already plotted in Fig. 3.

to the reservoir, and for some special values of k that are close to resonance. While in these plots for most momenta, the amplitude of higher Fourier modes are weaker than the lower Fourier modes, around resonances it is possible that this trend becomes reversed. For instance, Fig. 6 shows that for $k_x = 0.3$, which is close to a resonance, $|\rho^1_{du}|$ is greater than $|\rho^0_{du}|$. This enhancement of $n = 1$ photon processes is also visible in ρ^n_{du} plotted in Figs. 4 and 5 for $k_x \sim 0.5, 1.5$.

In order to understand how measurable quantities are affected, in Fig. 7 we plot the time-averaged spin density

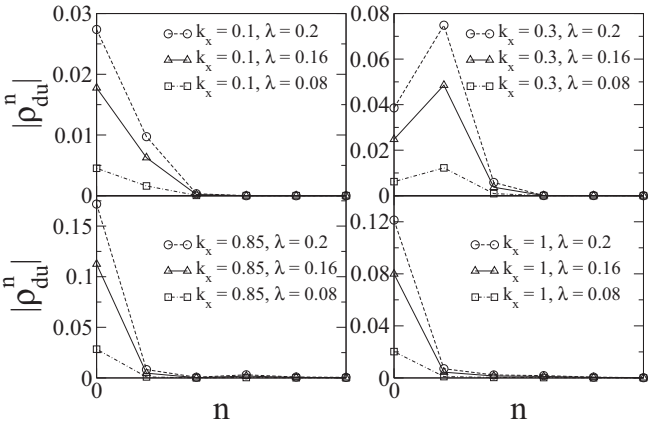

FIG. 6. Comparison of the off-diagonal Floquet occupation probabilities for three different coupling strengths to the reservoir: $\lambda/\Omega = 0.08, 0.16, 0.2$ and $T = 0.1\Omega$, $k_y = 0$. We have set $\Omega = 1.0$.

defined as $m_z(k) = \frac{1}{T_\Omega}\int_0^{T_\Omega} dt\, m_z(k,t)$ where

$$m_z(k,t) = \mathrm{Tr}\left[W_{\mathrm{el}}(t)\sum_\sigma \sigma c^\dagger_{k\sigma}c_{k\sigma}\right] = \sum_{\alpha,\beta=u,d}\left[\rho_{k,\alpha\beta}(t)\sum_\sigma \sigma\langle\phi_{k\beta}(t)|c^\dagger_{k\sigma}c_{k\sigma}|\phi_{k\alpha}(t)\rangle\right]. \tag{25}$$

Note that this quantity is zero in the absence of the drive, and a nonzero value of m_z is a consequence of the broken time-reversal symmetry under the influence of the circularly polarized laser. The momentum-resolved spin density can be measured in spin-resolved ARPES [37] (angle-resolved photoemission spectroscopy), an experimental technique capable of observing the distribution of electrons in a spin-resolved manner. This method for example has been used to show spin-momentum locking of the surface states of 3D topological insulators [40]. In an earlier paper, we discussed [20] the spin texture for the Floquet-Dirac system when only diagonal components of the density matrix are kept. With the inclusion

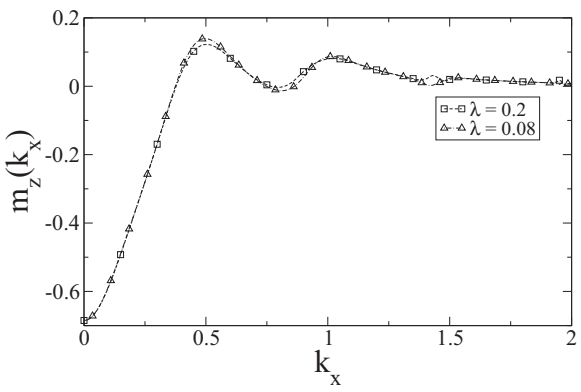

FIG. 7. Time-averaged spin density at steady state along $k_y = 0$ and for reservoir temperature $T = 0.1\Omega$. We have set $\Omega = 1.0$. The differences for different λ albeit small, are most pronounced near resonance ($k_x \sim 0.5, 1$).

of off-diagonal terms as done here, we find that a qualitatively new feature is a dependence of the results on the coupling strength to a reservoir. While this dependence is weak for the parameters we have chosen, near a topological phase transition, where the levels come even closer together, the reservoir dependence of m_z will become more enhanced.

As the coupling strength to the reservoir is increased, the diagonal component of the density matrix is not significantly affected, but the off-diagonal component is strongly affected, and increases with λ. We therefore coin the term "reservoir-induced coherence." This is unusual as typically in most open systems, the reduced density matrix is strongly dephased by coupling to a reservoir, making it approach a diagonal ensemble. Of course, one may always choose a time-dependent basis where the density matrix looks effectively diagonal. What we find here is not a trivial basis-dependent effect because the quantity which measures the purity of the density matrix $\mathrm{Tr}[(W_{\mathrm{el}})^2]$ increases in our model as coupling to the reservoir is increased. For a pure system $\mathrm{Tr}[(W_{\mathrm{el}})^2] = 1$, while for a mixed state $\mathrm{Tr}[(W_{\mathrm{el}})^2] < 1$. For our system $\mathrm{Tr}[(W_{\mathrm{el}})^2] = 2|\rho_{k,du}|^2 + 1 + 2\rho_{k,dd}(\rho_{k,dd} - 1)$. Thus, it is clear that if $\rho_{k,dd}$ is only weakly affected by λ (as shown in Fig. 3) while $|\rho_{k,du}|$ strongly increases with λ, it will lead to a purer state. In fact, as shown in Appendix C, an analytic calculation at the Dirac point ($k = 0$) can be done. Here, we find that for a weak laser field ($A_0/\Omega \ll 1$), and for a reservoir temperature that is small as compared to the quasienergy level spacing ($T \ll \sqrt{4A_0^2 + \Omega^2} - \Omega \sim 2A_0^2/\Omega$),

$$\rho_{dd} = 1 + \mathcal{O}\left(\frac{A_0}{\Omega}\mathrm{Re}[\rho_{du}]\right) = 1 + \mathcal{O}\left(\frac{\lambda^4\nu^2 A_0^2}{\Omega^4}\right). \quad (26)$$

Thus, the above confirms our observation of a very weak dependence of the diagonal component of the density matrix on the electron-reservoir coupling strength. In contrast as shown in Appendix C, the off-diagonal component (in particular, its imaginary part) is $\mathcal{O}(\lambda^2\nu A_0/\Omega^2)$, and depends much more sensitively on the coupling to the reservoir.

It is interesting to note that such reservoir-induced coherence has also been predicted in other driven-dissipative systems [41–43], where they are encountered when two or more two-level systems are coupled to the same reservoir. In such a situation, the reservoir can induce an effective entanglement between the two-level systems. In our model, similar physics is at play. Even though at each k we have a single two-level system corresponding to the sublattice of graphene or to the spin on the surface of a TI, the periodic drive introduces effectively many levels, the Floquet levels. Now, in our Floquet master equation, all the Floquet levels at a given k are coupled to the same phonon reservoir, resulting in a similar reservoir-induced entanglement or coherence between the Floquet levels. In the next section, we explicitly show that this enhanced coherence arises because the reservoir can absorb the excess entropy in the system, especially when there are reservoir density of states at multiples of the driving frequency.

It is convenient to define a decoherence measure for the steady state by $1 - \mathrm{Tr}[(W_{\mathrm{el}}^{\mathrm{SS}})^2]$. This decoherence measure vanishes for the pure state, and increases as the density matrix becomes more mixed. The decoherence is plotted in Fig. 8 for $\lambda/\Omega = 0.08, 0.16, 0.2$ and shows that the reservoir-induced coherence increases with λ, and is enhanced closer to resonances, with the possibility of complete coherence around $k_x \sim 1.42$. Such coherent states appearing out of dissipative coupling to the reservoir are also known as dark states [43].

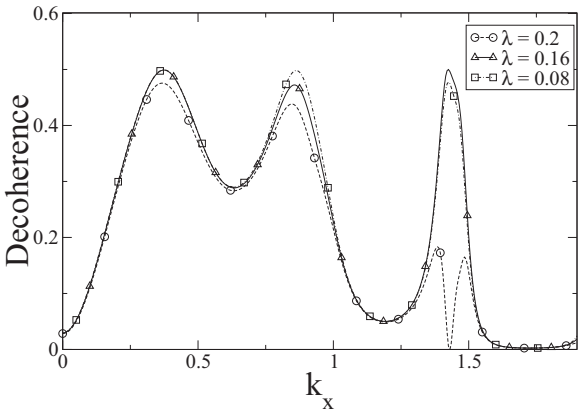

FIG. 8. Plot of steady-state decoherence measured as the time average of $1 - \mathrm{Tr}[(W_{\mathrm{el}})^2]$, for $\lambda/\Omega = 0.08, 0.16, 0.2$, with $\Omega = 1.0$, $T = 0.1\Omega$. The decoherence decreases as the coupling to the reservoir increases, with indication of a dark state around $k_x \sim 1.42$.

IV. STEADY-STATE ENTROPY-PRODUCTION RATE AND COHERENCE

The steady state generally does not coincide with a Gibbs distribution, where for the latter one would expect the following for the time-averaged distribution function $\rho_{k,uu}^{\mathrm{Gibbs}} = (e^{(\epsilon_{ku}-\epsilon_{kd})/T} + 1)^{-1}$, $\rho_{k,dd}^{\mathrm{Gibbs}} = 1 - \rho_{k,uu}^{\mathrm{Gibbs}}$, with T being the temperature of the reservoir. One may quantify this lack of detailed balance in the system in terms of an entropy-production rate [44,45]. Below we derive a general expression for it, and then apply it to our system.

For any time-dependent Hamiltonian, and for a time evolution from some initial time $t = 0$ to $t = \tau$, the first law of thermodynamics states that the mean work $\langle w \rangle$ performed during this interval, the mean heat $\langle Q \rangle$ exchanged with a reservoir at temperature $T = \beta^{-1}$ and the change in the internal energy ΔU of the system are related as

$$\Delta U = \langle w \rangle + \langle Q \rangle, \quad (27)$$

where $\Delta U = U_\tau - U_0$. The above is simply stating energy conservation.

The entropy at any given time is $s_t = -\mathrm{Tr}[W_{\mathrm{el}}(t) \ln W_{\mathrm{el}}(t)]$. The second law of thermodynamics states that the entropy is always greater than or equal to the heat exchanged with the reservoir. The amount by which the entropy is larger than the heat exchanged ($\Delta s - \beta\langle Q \rangle$) can be thought of as a net entropy production which is always non-negative. Thus, the mean entropy production over the time interval from $t = 0, \tau$ may be defined as

$$\Sigma = \Delta s - \beta\langle Q \rangle. \quad (28)$$

Using Eq. (27), this implies

$$\Sigma = \Delta s + \beta\langle w \rangle - \beta\Delta U. \quad (29)$$

Now, we give a quick derivation of the entropy-production rate $\partial_t \Sigma$, as outlined in Ref. [45].

We start with microscopic definitions of the internal energy and the mean work in terms of the density matrix. The internal energy is given by

$$U_t = \mathrm{Tr}[W_{\mathrm{el}}(t) H_{\mathrm{el}}(t)]. \tag{30}$$

The average work done $\langle w \rangle$ during a time interval from 0 to τ may be written as [45]

$$\langle w \rangle = \int_0^\tau dt\, \mathrm{Tr}[W_{\mathrm{el}}(t) \partial_t H_{\mathrm{el}}(t)]. \tag{31}$$

Let us also define a density matrix representing an ideal Gibbs state at time t:

$$W_{\mathrm{el}}^{\mathrm{eq}}(t) = \frac{e^{-\beta H_{\mathrm{el}}(t)}}{Z_t}; \quad Z_t = \mathrm{Tr}[e^{-\beta H_{\mathrm{el}}(t)}]. \tag{32}$$

The entropy-production rate can be obtained from differentiating Eq. (29) with time. Note that the rate of change of the entropy is given by

$$\dot{s}(t) = -\mathrm{Tr}[\dot{W}_{\mathrm{el}}(t) \ln W_{\mathrm{el}}(t)], \tag{33}$$

where we have used that $\partial_t \mathrm{Tr}[W_{\mathrm{el}}(t)] = \mathrm{Tr}[\partial_t W_{\mathrm{el}}(t)] = 0$. In the above and in the remainder, an overdot denotes a time derivative as in $\dot{W}_{\mathrm{el}}(t) = \partial_t W_{\mathrm{el}}(t)$.

The change in the internal energy U in time has two contributions, one from the change in the distribution function W_{el} with time, and the second from changes to the Hamiltonian $H_{\mathrm{el}}(t)$ with time. Identifying the latter as the rate at which work is done,

$$\beta \partial_t [\langle w \rangle - U] = -\beta\, \mathrm{Tr}[\dot{W}_{\mathrm{el}}(t) H_{\mathrm{el}}(t)]. \tag{34}$$

One immediately obtains from Eqs. (29), (33), and (34)

$$\dot{\Sigma} = -\mathrm{Tr}\left[\dot{W}_{\mathrm{el}} \ln \frac{W_{\mathrm{el}}(t)}{W_{\mathrm{el}}^{\mathrm{eq}}(t)}\right]. \tag{35}$$

Equation (35) shows that the entropy-production rate is zero when either $\dot{W}_{\mathrm{el}}(t) = 0$ (i.e., the system has reached a time-independent steady state) and/or detailed balance is obeyed in that the distribution function equals the Gibbs distribution $W_{\mathrm{el}}(t) = W_{\mathrm{el}}^{\mathrm{eq}}(t)$. We will now show that the steady state in a Floquet system, where the density matrix has synchronized with the laser, is characterized by a net entropy-production rate, which also increases with coupling to the reservoir.

A useful quantity is the entropy-production rate averaged over one cycle of the laser. Since at steady state, due to synchronization, $W_{\mathrm{el}}^{\mathrm{SS}}(t) = W_{\mathrm{el}}^{\mathrm{SS}}(t + T_\Omega)$, the time average vanishes:

$$\frac{1}{T_\Omega} \int_0^{T_\Omega} dt\, \mathrm{Tr}\big[\dot{W}_{\mathrm{el}}^{\mathrm{SS}} \ln W_{\mathrm{el}}^{\mathrm{SS}}(t)\big] = 0. \tag{36}$$

Thus, the time-averaged entropy-production rate simplifies to

$$\overline{\dot{\Sigma}^{\mathrm{SS}}} = -\frac{\beta}{T_\Omega} \int_0^{T_\Omega} dt\, \mathrm{Tr}\big[\dot{W}_{\mathrm{el}}^{\mathrm{SS}} H_{\mathrm{el}}(t)\big], \tag{37}$$

where an overline denotes time averaging over one cycle.

To clarify the meaning of the entropy-production rate in the steady state, we note that the time-averaged rate of change of the entropy vanishes due to the time periodicity of the density matrix:

$$\begin{aligned} \overline{\dot{s}^{\mathrm{SS}}} &= -\frac{1}{T_\Omega} \int_0^{T_\Omega} dt\, \mathrm{Tr}\big[\dot{W}_{\mathrm{el}}^{\mathrm{SS}} \ln W_{\mathrm{el}}^{\mathrm{SS}}(t)\big] \\ &= 0. \end{aligned} \tag{38}$$

Similarly, one can show that $\overline{\dot{U}^{\mathrm{SS}}} = 0$. Therefore, from Eq. (29), in the steady state one finds

$$\overline{\dot{\Sigma}^{\mathrm{SS}}} = \beta \overline{\langle \dot{w}^{\mathrm{SS}} \rangle} \tag{39}$$

or, equivalently,

$$\overline{\dot{\Sigma}^{\mathrm{SS}}} = -\beta \overline{\langle \dot{Q}^{\mathrm{SS}} \rangle}. \tag{40}$$

Therefore, in the steady state, a nonvanishing entropy-production rate is equivalent to the heat current flowing out of the system and into the reservoir. Since according to the second law of thermodynamics the entropy production is always non-negative, when this quantity is nonzero, it implies that the work performed on the system cannot be absorbed in the internal energy of the system. This energy is converted into heat and flows out of the system towards the reservoir.

We have proved in Appendix B that in the steady state where the density matrix synchronizes with the periodic drive, the entropy-production rate can be expressed as follows in terms of the components of the density matrix and the quasimodes:

$$\overline{\dot{\Sigma}^{\mathrm{SS}}} = -\beta \sum_{\alpha,\beta} \overline{\langle \phi_{k,\beta}(t) | \dot{\phi}_{k,\alpha}(t) \rangle (\epsilon_{k\beta} - \epsilon_{k\alpha} + i\partial_t) \rho_{k,\alpha\beta}^{\mathrm{SS}}}. \tag{41}$$

We note that the above quantity is real, and also independent of the gauge, i.e., it does not depend on the arbitrariness in choosing the quasimodes and quasienergies (see Appendix B for a discussion of this point). In addition, we find that the result depends weakly on the diagonal components of the density matrix and it is mainly controlled by the off-diagonal components of the density matrix. While we can show this analytically at $k = 0$, for nonzero k, this is an observation from our numerical simulations. Thus, after ignoring the oscillations of the diagonal elements of the density matrix, and for a two-level system, one finds

$$\overline{\dot{\Sigma}^{\mathrm{SS}}} \simeq 2\beta \mathrm{Re}\left[\overline{\big((\epsilon_{ku} - \epsilon_{kd}) \rho_{k,du}^{\mathrm{SS}} + i \dot{\rho}_{k,du}^{\mathrm{SS}}\big) \langle \dot{\phi}_{k,u}(t) | \phi_{k,d}(t) \rangle}\right]. \tag{42}$$

It is interesting to note that if we had made the commonly employed Floquet-Markov approximation [35] which involves replacing the rates by their time-averaged values, then by construction $\dot{\rho}_{k,du}^{\mathrm{SS}} = 0$, and in that case the above expression for the entropy-production rate would have been gauge dependent and hence unphysical. Thus, by keeping the full time dependence of the rates, we have a correct measure of how non-Gibbsian the resulting steady state is.

Now, let us turn to an analytic study for the entropy-production rate at $k = 0$. In Appendix C, we showed that for a certain convenient gauge choice $\partial_t \rho_{k=0,du}^{\mathrm{SS}} = 0$. Moreover, independent of the gauge $\partial_t \rho_{k=0,dd}^{\mathrm{SS}} = 0$. In this case, one finds that the entropy-production rate is

$$\overline{\dot{\Sigma}^{\mathrm{SS}}}(k = 0) = 2\beta A_0 \Omega\, \mathrm{Im}\big[\rho_{k=0,du}^{\mathrm{SS}}\big]. \tag{43}$$

Thus, at the Dirac point, the entropy-production rate is proportional to the magnitude of the off-diagonal component of the density matrix, and an electric field due to the laser given by the combination $A_0\Omega$. An analytic expression may be obtained for the off-diagonal component. While originally to simplify the numerical calculations, we assumed a model with energy-independent electron-phonon coupling and density of states, at $k = 0$ we can restore the energy dependence of these parameters. When $A_0/\Omega \ll 1$, we find

$$\mathrm{Im}[\rho_{k=0,du}] = \frac{\left(2\lambda_\Omega^2 \nu_\Omega\right) A_0}{\Omega^2 + (2\lambda_-^2 \nu_-)^2 [1 + 2N_-]^2}, \tag{44}$$

where the subscripts Ω and $-$ in λ and ν denote the value of these quantities at energy Ω and energy equal to the topological gap $\Omega_- = \Delta - \Omega \approx 2A_0^2/\Omega$, respectively. Therefore, by tracing back the origins of the interactions, one can detect the corresponding microscopic processes which produce coherence. For $A_0/\Omega \ll 1$, the main processes responsible for creation of off-diagonal components and therefore coherence are the Floquet-umklapp processes during which electrons are allowed to absorb or emit phonons with energy Ω from or into the reservoir. This explains the presence of $\lambda_\Omega^2 \nu_\Omega$ in the numerator of Eq. (44).

By detecting the dominant interaction one can engineer the reservoir so as to increase coherence. Here, this is realized by enhancing the density of states of phonons or the coupling constant at energy Ω. Thus, as the drive pumps energy at Ω, the system can stay coherent by releasing this energy into the reservoir.

The denominator of Eq. (44) also shows that the dissipation due to the reservoir phonons at the gap energy Ω_- measured by the coupling $\lambda_-^2 \nu_-$ is enhanced by the Bose factor $(1 + 2N_-)$. Note that the laser-induced gap at the Dirac point is of the order of 100 meV in most currently accessible setups [37]. At temperatures that are small as compared to this gap ($\beta A_0^2/\Omega \gg 1$),

$$\mathrm{Im}[\rho_{k=0,du}] \sim \nu_\Omega \lambda_\Omega^2 \frac{A_0}{\Omega^2}, \tag{45}$$

so that

$$\overline{\dot{\Sigma}^{\mathrm{SS}}}(k = 0, A_0/\Omega \ll 1) \sim \beta(A_0\Omega)\left(\nu_\Omega \frac{\lambda_\Omega^2}{\Omega}\right)\frac{A_0}{\Omega} \tag{46}$$

or, equivalently from Eq. (38),

$$\overline{\dot{Q}^{\mathrm{SS}}}(k = 0, A_0/\Omega \ll 1) \sim -(A_0\Omega)\left(\nu_\Omega \frac{\lambda_\Omega^2}{\Omega}\right)\frac{A_0}{\Omega}. \tag{47}$$

Thus, for low field amplitudes and low temperatures, the heat-production rate increases with the effective electric field $A_0\Omega$, and is constant as a function of the temperature.

For nonzero k, where analytic computations are not possible anymore, our numerical results for the steady-state entropy and entropy-production rate are presented in Figs. 9 and 10, respectively. Figure 9 shows that by increasing the coupling constant, the time-averaged entropy decreases. However, since the entropy is determined mainly by the diagonal components of the density matrix which are not sensitive to the coupling constant, the difference between different curves is small and is only significant around the resonances. This decrease in the entropy can be interpreted effectively as a band-gap opening induced by the electron-phonon coupling [35] analogous to avoided level crossings caused by external perturbations.

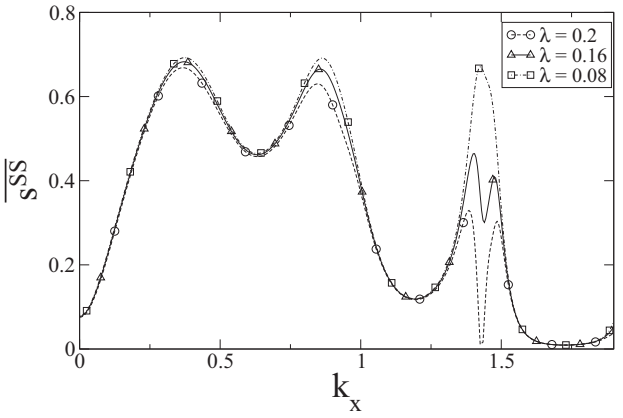

FIG. 9. Plot of the steady-state entropy after time averaging, for three different electron-phonon coupling strengths $\lambda/\Omega = 0.08, 0.16, 0.2$ and phonon temperature $T = 0.1\Omega$. We have set $\Omega = 1.0$. The entropy decreases with increasing strength of the coupling to the reservoir.

Figure 10 shows the time-averaged entropy-production rate for different momenta and three different strengths of the coupling to the reservoir. As the reservoir coupling increases, the steady-state entropy-production rate increases, indicating a larger deviation from detailed balance. Recalling that the entropy-production rate is proportional to the heat released by the system, one naturally expects that by strengthening the coupling of the system to the reservoir, the outward heat generated by the system must increase. Note that this figure has the same structure as Fig. 9 with an enhancement near resonances. However, unlike Fig. 9, in Fig. 10 the curves are much more sensitive to the change in the coupling constant. This stems from the fact that, as proved in Appendix B,

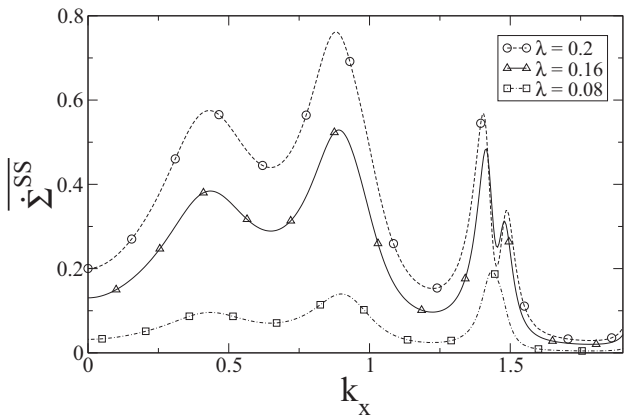

FIG. 10. The steady-state entropy-production rate time averaged over a laser cycle, along $k_y = 0$ for three different electron-phonon couplings $\lambda/\Omega = 0.08, 0.16, 0.2$. The phonon temperature is $T = 0.1\Omega$. We have set $\Omega = 1.0$. The entropy-production rate increases as coupling to the reservoir is increased. This is accompanied by a decreasing decoherence (Fig. 8) and decreasing system entropy (Fig. 9).

the heat rate or entropy-production rate depends mainly on the off-diagonal components of the density matrix, while the entropy depends mostly on the diagonal components, where the latter are not very sensitive to the coupling constant. This also implies that a small decrease in the steady-state entropy is compensated by a considerable amount of heat released by the system into the reservoir.

V. CONCLUSIONS

We have studied an open Floquet topological system under the assumption that the reservoir to which the system is coupled is Markovian. The topology in the system arises because the circularly polarized laser opens up a gap at the Dirac points whose origin is the breaking of time-reversal symmetry in the Floquet Hamiltonian, with the quasienergy bands acquiring a nonzero Berry curvature.

The combination of periodic drive and dissipation gives rise to many results. One of them is an effective reservoir-induced coherence. This comes about if there are reservoir density of states at the laser frequency, or some multiples of it. For such a case, as the drive pumps energy into the system, the system can give up this energy to the reservoir. In particular, this coherence arises due to Floquet-umklapp processes that allow the electron to release energy at multiples of the drive without causing transitions between distinct electronic states, where the latter processes would be akin to decoherence.

The signature of this coherence is a nonzero off-diagonal matrix element in the Floquet basis that grows with the strength of the coupling to the reservoir, while the diagonal component is only weakly affected by the coupling strength to the reservoir. This has the effect of increasing the purity of the steady-state density matrix, measured by $\mathrm{Tr}[W_{\mathrm{el}}^2]$.

The second important result is a steady state that is in general not a Gibbs distribution. We characterize this lack of detailed balance by a net steady-state entropy-production rate. We have shown that a nonzero entropy production mostly depends on the off-diagonal components of the density matrix. Since in the steady state an entropy-production rate is equivalent to the heat released by the system, this result can be used to engineer the phonon reservoir such that the system can efficiently give up heat to the reservoir, becoming more coherent. Furthermore, we find that the entropy-production rate increases with coupling to the reservoir, and also when one is closer to resonances, where the quasienergy level spacings become small.

Due to the synchronization of the system, we extract explicit results for the occupation probabilities of the Floquet levels from a Fourier decomposition of the steady-state density matrix. We show that in the vicinity of resonances, not only do the off-diagonal elements become stronger, but more number of Floquet quasienergy levels are occupied.

All the above results are supplemented by exact analytic expressions at the Dirac point which highlight the complex interplay of the many energy scales in the problem: system-reservoir coupling, reservoir temperature, frequency of the laser, amplitude of the laser, and quasienergies. Consequently, one can use these different energy scales to find a criterion to maximize coherence. The results for the Floquet occupation probabilities, and in particular their dependence on the strength of the system-reservoir coupling, can be tested in experiments such as time-resolved and spin-resolved ARPES.

At this point, a note of caution is in order. We find that the Markovian approximation that relies on a weak coupling to the reservoir breaks down for large momentum and for very small level crossings relative to the coupling to the reservoir. For our parameters, this happens near $k_x \sim 2$ and couplings greater than $\lambda/\Omega \sim 0.25$, where the density matrix starts acquiring negative eigenvalues. In such a case, more sophisticated methods which treat the reservoir nonperturbatively are needed.

Floquet topological phase transitions are characterized by jumps in the Chern number. However, the transitions when measured in terms of observables such as the Hall conductance will show rounding [20], with the extent of rounding depending not only on the temperature of the reservoir, but also on the strength of the coupling to the reservoir. A proper theory for Floquet topological phase transitions for the open system will need to account for the subtleties discussed in this paper.

One of the key observations of our paper is that if reservoir density of states exists at multiples of the drive frequency, then very efficient cooling is possible, with the system at steady state becoming more coherent than a Gibbs state at the temperature of the reservoir. An interesting question would be to explore how the reservoir coupling can be further engineered to make the system reach dark states which correspond to completely pure states with $\mathrm{Tr}[W_{\mathrm{el}}^2] = 1$.

ACKNOWLEDGMENTS

The authors thank A. Clerk, J. Keeling, S. Kehrein, I. Martin, and R. K. P. Zia for helpful discussions. This work was supported by the US Department of Energy, Office of Science, Basic Energy Sciences, under Award No. DE-SC0010821.

APPENDIX A: SYNCHRONIZATION OF THE STEADY-STATE DENSITY MATRIX

We show in this appendix that after reaching the steady state, the density matrix harmonizes with the external drive in the Schrödinger picture. While in our numerical simulation we use a time-dependent R matrix, in this appendix we use a time-averaged rate matrix which will simplify the proof. We start with the Floquet master equation (18) which consists of four complex equations for the components of the density matrix. To represent these equations in a matrix form, we form a column vector from the components of the density matrix

$$\vec{\boldsymbol{\rho}}_k^D(t) = \begin{pmatrix} \rho_{k,dd}(t) \\ \rho_{k,du}(t) \\ \rho_{k,ud}(t) \\ \rho_{k,uu}(t) \end{pmatrix}. \tag{A1}$$

Now, the Floquet master equation can be represented in matrix form

$$\dot{\vec{\boldsymbol{\rho}}}_k^D(t) = \boldsymbol{L}_k^D(t)\vec{\boldsymbol{\rho}}_k^D(t), \tag{A2}$$

where $\boldsymbol{L}_k^D(t)$ is a 4×4 matrix which can be read off from Eq. (18). Not all of the components of the above vector denoted in our notation by the superscript D in $\vec{\boldsymbol{\rho}}_k^D$ are independent. To find the linearly independent components of the density matrix, note that the diagonal components of the density matrix are

purely real and must satisfy

$$\rho_{k,dd} + \rho_{k,uu} = 1. \tag{A3}$$

To preserve this conservation equation, one of the eigenvalues of $\boldsymbol{L}_k^D(t)$ must be always equal to zero. Equivalently, we can remove one of the diagonal components of the density matrix, e.g., $\rho_{k,uu} = 1 - \rho_{k,dd}$. Moreover, since the density matrix is Hermitian, this requires $\rho_{k,du} = \rho_{k,ud}^*$. Thus, we can define a linearly independent density vector consisting of three components as in the following:

$$\vec{\boldsymbol{\rho}}_k(t) = \begin{pmatrix} \rho_{k,dd}(t) \\ \rho_{k,du}(t) \\ \rho_{k,du}^*(t) \end{pmatrix}. \tag{A4}$$

Eventually, one can rewrite Eq. (A2) in terms of the independent components

$$\dot{\vec{\boldsymbol{\rho}}}_k(t) = \boldsymbol{L}_k(t)\vec{\boldsymbol{\rho}}_k(t) + \vec{\boldsymbol{b}}_k(t). \tag{A5}$$

Above $\boldsymbol{L}_k(t)$ is a 3×3 time-dependent matrix which is formed by the rate matrix $R_{\alpha\beta,\gamma\delta}$ and the quasienergy difference. We can separate these into two contributions

$$\boldsymbol{L}_k(t) = \boldsymbol{L}_k^R(t) + \boldsymbol{L}_k^\epsilon, \tag{A6}$$

where

$$\boldsymbol{L}_k^\epsilon = \begin{pmatrix} 0 & 0 & 0 \\ 0 & i(\epsilon_u - \epsilon_d) & 0 \\ 0 & 0 & i(\epsilon_d - \epsilon_u) \end{pmatrix} \tag{A7}$$

is purely imaginary and $\boldsymbol{L}_k^R(t)$ is only composed of $R^k_{\alpha\beta,\gamma\delta}$. Here, we do not need the explicit form of this matrix. In Eq. (A5), $\vec{\boldsymbol{b}}_k(t)$ is a three-component column vector which originates from replacing $\rho_{k,uu}$ by $1 - \rho_{k,dd}$.

Here, we mention some of the properties of $\boldsymbol{L}_k^R(t)$ and $\vec{\boldsymbol{b}}_k(t)$ which will be used. The first property is that since these two quantities are obtained from the components of the $R_{\alpha\beta,\gamma\delta}$ matrix, they can at most have a periodic dependence on time. The second property has to do with the eigenvalues of the $\boldsymbol{L}_k(t)$ matrix. These can at most have real parts that are negative, which ensure stable solutions where components of the density matrix are confined ($0 \leqslant \rho_{k,dd} \leqslant 1$, $|\rho_{k,du}| \leqslant 1/2$), and there is no exponential growth in time. This can be understood by considering the closed solutions of Eq. (A5):

$$\vec{\boldsymbol{\rho}}_k(t) = e^{\int_0^t dt_3 \boldsymbol{L}_k(t_3)}\left(\vec{\boldsymbol{\rho}}_k(0) + \int_0^t dt_1 e^{-\int_0^{t_1} dt_2 \boldsymbol{L}_k(t_2)}\vec{\boldsymbol{b}}_k(t_1)\right). \tag{A8}$$

Now, we plan to use the above information to study the asymptotic behavior of the solutions of the density matrix. However, as one can see in the above formula, without knowing the explicit time dependence of $\boldsymbol{L}_k(t)$, we cannot yet compute this integral. To overcome this we consider the case where it is a permissible approximation to replace $\boldsymbol{L}_k(t)$ with its mean value. This requires that the temporal oscillations of $\boldsymbol{L}_k(t)$ around its mean value be comparatively small, which corresponds to small electron-phonon coupling constants and momentum. In such cases, one can verify by numerical simulations that the steady-state solutions of the original Floquet master equation with a time-dependent rate matrix, after averaging over time, yields the same answer as the solutions of the time-averaged Floquet master equation with $\overline{\boldsymbol{L}}_k$. Therefore, before considering the more general case we will consider a time-averaged master equation.

After replacing $\boldsymbol{L}_k(t)$ and $\vec{\boldsymbol{b}}_k(t)$ with their time-averaged values, we can calculate the time integrals explicitly

$$\vec{\boldsymbol{\rho}}_k(t) = e^{t\overline{\boldsymbol{L}}_k}\left(\vec{\boldsymbol{\rho}}_k(0) + \int_0^t dt_1 e^{-t_1\overline{\boldsymbol{L}}_k}\overline{\vec{\boldsymbol{b}}}_k\right). \tag{A9}$$

In the steady state, the first term in the above becomes infinitesimally small at long times because the eigenvalues of $\overline{\boldsymbol{L}_k}$ have negative real parts. Thus,

$$\lim_{t\to\infty} \vec{\boldsymbol{\rho}}_k(t) = \lim_{t\to\infty} e^{t\overline{\boldsymbol{L}}_k}\int_0^t dt_1 e^{-t_1\overline{\boldsymbol{L}}_k}\overline{\vec{\boldsymbol{b}}}_k. \tag{A10}$$

We can compute the integrals and obtain

$$\lim_{t\to\infty} \vec{\boldsymbol{\rho}}_k(t) = \lim_{t\to\infty} \overline{\boldsymbol{L}}_k^{-1}(e^{t\overline{\boldsymbol{L}}_k} - 1)\overline{\vec{\boldsymbol{b}}}_k = -\overline{\boldsymbol{L}}_k^{-1}\overline{\vec{\boldsymbol{b}}}_k. \tag{A11}$$

Therefore, in the steady state with a time averaged $\overline{\boldsymbol{L}}_k$ the density matrix asymptotically becomes constant in time and the oscillations with the frequency $\epsilon_{ku} - \epsilon_{kd}$ fade out. Let us highlight that this result does not depend on the specific form of the reservoir coupling.

After showing that the nonharmonic oscillations with $\epsilon_{ku} - \epsilon_{kd}$ vanish in a time-averaged Floquet master equation, one can argue that in the time-dependent Floquet master equation such oscillations must vanish as well and one can only have harmonic solutions with frequency Ω. This can be realized by using the Floquet theorem for differential equations. Very briefly, this theorem states that the solution of a homogeneous linear differential equation with a periodic matrix, as in the time-dependent master equation (A2), is given by $\vec{\boldsymbol{\rho}}_k^D(t) = \phi_k(t)\vec{\boldsymbol{\rho}}_k^D(0)$, where $\phi_k(t)$ is the fundamental solution of this differential equation which can be decomposed as $\phi_k(t) = P_k(t)e^{tB_k}$ with $P_k(t)$ a periodic in time matrix and B_k a time-independent matrix [46]. As in $\boldsymbol{L}_k^D(t)$, one of the eigenvalues of B_k must always vanish so as to preserve the conservation law of probabilities. Moreover, similar to the above discussion for the time averaged $\overline{\boldsymbol{L}}_k$, one can argue that the other three eivenvalues of B_k must have negative real parts. Therefore, at long times, e^{tB_k} will asymptotically become constant, and therefore only the periodic part of the fundamental solution will survive [35]. This proves our claim for a Floquet master equation with periodic in time rates.

APPENDIX B: STEADY-STATE ENTROPY-PRODUCTION RATE

Here, we plan to derive an expression for the steady-state entropy-production rate, namely Eq. (41). Let us start from the following expression derived in the main text:

$$\dot{\Sigma} = -\mathrm{Tr}\left[\dot{W}_{\mathrm{el}} \ln\left(\frac{W_{\mathrm{el}}}{W_{\mathrm{el}}^{\mathrm{eq}}}\right)\right], \tag{B1}$$

where

$$W_{\mathrm{el}}^{\mathrm{eq}} = \frac{e^{-\beta H_{\mathrm{el}}(t)}}{Z_t}, \quad Z_t = \mathrm{Tr}[e^{-\beta H_{\mathrm{el}}(t)}], \tag{B2}$$

$H_{\rm el}(t)$ denotes the time-dependent Hamiltonian of the system. We can simplify Eq. (B1) by expanding the logarithm

$$\dot{\Sigma} = -\mathrm{Tr}[\dot{W}_{\rm el} \ln W_{\rm el}] - \mathrm{Tr}[\beta H_{\rm el}(t)\dot{W}_{\rm el}] - (\ln Z_t)\mathrm{Tr}[\dot{W}_{\rm el}]. \tag{B3}$$

We are only interested in the average of the entropy-production rate at steady state where the density matrix synchronizes with the external drive, and the density matrix in the Schrödinger picture is

$$W^{\rm SS}_{\rm el}(t) = \sum_{\alpha,\beta} \rho^{\rm SS}_{k,\alpha\beta} |\phi_{k,\alpha}(t)\rangle\langle\phi_{k,\beta}(t)|. \tag{B4}$$

As we have shown in Appendix A, in the Schrödinger picture all the components of $\rho^{\rm SS}_{k,\alpha\beta}$, including the off-diagonal components, are periodic in the steady state. As the Floquet quasimodes are periodic too, one finds $W^{\rm SS}_{\rm el}(t+T_\Omega) = W^{\rm SS}_{\rm el}(t)$. Consequently, by periodicity of $W^{\rm SS}_{\rm el}$ we find that on time averaging Eq. (B3) over a cycle of the laser,

$$\overline{\dot{\Sigma}^{\rm SS}} \equiv \frac{1}{T_\Omega}\int_0^{T_\Omega} \dot{\Sigma}^{\rm SS} dt = -\beta\,\mathrm{Tr}\big[\overline{H_{\rm el}(t)\dot{W}^{\rm SS}_{\rm el}(t)}\big]. \tag{B5}$$

The time derivative of the density matrix in the Schrödinger picture is

$$\dot{W}^{\rm SS}_{\rm el} = \sum_{\alpha,\beta}\big[\dot{\rho}^{\rm SS}_{k,\alpha\beta}|\phi_{k,\alpha}(t)\rangle\langle\phi_{k,\beta}(t)| + \rho^{\rm SS}_{k,\alpha\beta}|\dot{\phi}_{k,\alpha}(t)\rangle\langle\phi_{k,\beta}(t)| + \rho^{\rm SS}_{k,\alpha\beta}|\phi_{k,\alpha}(t)\rangle\langle\dot{\phi}_{k,\beta}(t)|\big]. \tag{B6}$$

To proceed, we must compute the trace in Eq. (B5). Note that with an arbitrary operator A, and arbitrary vectors u and v, the definition of tracing gives

$$\mathrm{Tr}[H_{\rm el}(t)|u\rangle\langle v|] = \langle v|H_{\rm el}(t)|u\rangle. \tag{B7}$$

This simplifies Eq. (B5):

$$\overline{\dot{\Sigma}^{\rm SS}} = -\beta\sum_{\alpha,\beta}\frac{1}{T_\Omega}\int_0^{T_\Omega} dt\big[\dot{\rho}^{\rm SS}_{k,\alpha\beta}\langle\phi_{k,\beta}(t)|H_{\rm el}(t)|\phi_{k,\alpha}(t)\rangle + \rho^{\rm SS}_{k,\alpha\beta}\langle\phi_{k,\beta}(t)|H_{\rm el}(t)|\dot{\phi}_{k,\alpha}(t)\rangle + \rho^{\rm SS}_{k,\alpha\beta}\langle\dot{\phi}_{k,\beta}(t)|H_{\rm el}(t)|\phi_{k,\alpha}(t)\rangle\big]. \tag{B8}$$

The action of the Hamiltonian on Floquet states can be computed by using the definition of the Floquet Hamiltonian

$$H^F_{\rm el} = H_{\rm el}(t) - i\partial_t. \tag{B9}$$

More explicitly, this gives

$$\begin{aligned} H_{\rm el}(t)|\phi_{k,\alpha}(t)\rangle &= H^F_{\rm el}|\phi_{k,\alpha}(t)\rangle + i\partial_t|\phi_{k,\alpha}(t)\rangle \\ &= \epsilon_{k\alpha}|\phi_{k,\alpha}(t)\rangle + i|\dot{\phi}_{k,\alpha}(t)\rangle, \end{aligned} \tag{B10}$$

and its complex conjugate

$$\langle\phi_{k,\alpha}(t)|H_{\rm el}(t) = \langle\phi_{k,\alpha}(t)|\epsilon_{k\alpha} - i\langle\dot{\phi}_{k,\alpha}(t)|. \tag{B11}$$

We can insert these relations in Eq. (B8). Let us consider each term in this equation separately. The first term becomes

$$\begin{aligned} \overline{\dot{\Sigma}^{\rm SS}_1} &\equiv -\beta\sum_{\alpha,\beta}\frac{1}{T_\Omega}\int_0^{T_\Omega} dt\,\dot{\rho}^{\rm SS}_{k,\alpha\beta}\langle\phi_{k,\beta}(t)|H_{\rm el}(t)|\phi_{k,\alpha}(t)\rangle \\ &= -\beta\sum_{\alpha,\beta}\big[\epsilon_{k\alpha}\delta_{\alpha\beta}\overline{\dot{\rho}^{\rm SS}_{k,\alpha\beta}} + i\,\overline{\rho^{\rm SS}_{k,\alpha\beta}\langle\phi_{k,\beta}(t)|\dot{\phi}_{k,\alpha}(t)\rangle}\big] \\ &= -\beta\sum_{\alpha,\beta} i\,\overline{\rho^{\rm SS}_{k,\alpha\beta}\langle\phi_{k,\beta}(t)|\dot{\phi}_{k,\alpha}(t)\rangle}, \end{aligned} \tag{B12}$$

where in the last equality we have used that $\overline{\dot{\rho}^{\rm SS}_{k,\alpha\beta}}$ vanishes because in the steady state the density matrix is periodic, and its time-averaged value is constant. Thus, the time derivative of the average vanishes. The second and third terms in Eq. (B8) are, respectively, given by

$$\begin{aligned} \overline{\dot{\Sigma}^{\rm SS}_2} &\equiv -\beta\sum_{\alpha,\beta}\frac{1}{T_\Omega}\int_0^{T_\Omega} dt\,\rho^{\rm SS}_{k,\alpha\beta}\langle\phi_{k,\beta}(t)|H_{\rm el}(t)|\dot{\phi}_{k,\alpha}(t)\rangle \\ &= -\beta\sum_{\alpha,\beta}\frac{1}{T_\Omega}\int_0^{T_\Omega} dt \\ &\quad\times\big[\epsilon_{k\beta}\rho^{\rm SS}_{k,\alpha\beta}\langle\phi_{k,\beta}(t)|\dot{\phi}_{k,\alpha}(t)\rangle - i\rho^{\rm SS}_{k,\alpha\beta}\langle\dot{\phi}_{k,\beta}(t)|\dot{\phi}_{k,\alpha}(t)\rangle\big] \end{aligned} \tag{B13}$$

and

$$\begin{aligned} \overline{\dot{\Sigma}^{\rm SS}_3} &\equiv -\beta\sum_{\alpha,\beta}\frac{1}{T_\Omega}\int_0^{T_\Omega} dt\,\rho^{\rm SS}_{k,\alpha\beta}\langle\dot{\phi}_{k,\beta}(t)|H_{\rm el}(t)|\phi_{k,\alpha}(t)\rangle \\ &= -\beta\sum_{\alpha,\beta}\frac{1}{T_\Omega}\int_0^{T_\Omega} dt \\ &\quad\times\big[\epsilon_{k\alpha}\rho^{\rm SS}_{k,\alpha\beta}\langle\dot{\phi}_{k,\beta}(t)|\phi_{k,\alpha}(t)\rangle + i\rho^{\rm SS}_{k,\alpha\beta}\langle\dot{\phi}_{k,\beta}(t)|\dot{\phi}_{k,\alpha}(t)\rangle\big]. \end{aligned} \tag{B14}$$

By summing the last two equations, terms with opposite signs cancel, and we obtain

$$\overline{\dot{\Sigma}^{\rm SS}_2} + \overline{\dot{\Sigma}^{\rm SS}_3} = -\beta\sum_{\alpha,\beta}(\epsilon_{k\beta} - \epsilon_{k\alpha})\overline{\rho^{\rm SS}_{k,\alpha\beta}\langle\phi_{k,\beta}(t)|\dot{\phi}_{k,\alpha}(t)\rangle}, \tag{B15}$$

where in the last equation we have used that $\partial_t\langle\phi_{k,\alpha}(t)|\phi_{k,\beta}(t)\rangle = 0$, so that

$$\langle\dot{\phi}_{k,\alpha}(t)|\phi_{k,\beta}(t)\rangle = -\langle\phi_{k,\alpha}(t)|\dot{\phi}_{k,\beta}(t)\rangle. \tag{B16}$$

Compiling the results from Eqs. (B15) and (B12), we find

$$\overline{\dot{\Sigma}^{\rm SS}} = -\beta\sum_{\alpha,\beta}\overline{\langle\phi_{k,\beta}(t)|\dot{\phi}_{k,\alpha}(t)\rangle(\epsilon_{k\beta} - \epsilon_{k\alpha} + i\partial_t)\rho^{\rm SS}_{k,\alpha\beta}}. \tag{B17}$$

It is straightforward to check that the right-hand side of Eq. (B17) is a purely real quantity.

Before using this result for a two-level system, we must explain some of its properties. First, note that since the entropy-production rate is a physical quantity, the left-hand side of this equation must be gauge invariant. Recall that while the Floquet quasimodes and quasienergies are not unique, the Schrödinger wave functions which are given by

$$|\psi_{k\alpha}(t)\rangle = e^{-i\epsilon_{k\alpha}t}|\phi_{k\alpha}\rangle \tag{B18}$$

are invariant under the following gauge transformations:

$$|\phi_{k\alpha}(t)\rangle \ \rightarrow e^{im_\alpha\Omega t}|\phi_{k\alpha}(t)\rangle, \tag{B19}$$

$$\epsilon_{k\alpha} \ \rightarrow \epsilon_{k\alpha} + m_\alpha\Omega, \tag{B20}$$

where m_α is an integer. Any physical observable is obtained from taking a trace with the density matrix $W_{\rm el}$. Since the result should be gauge invariant, this requires that under the above transformations, $\rho_{\alpha\beta}$ must transform as

$$\rho_{\alpha\beta} \ \rightarrow e^{-i(m_\alpha-m_\beta)\Omega t}\rho_{\alpha\beta}. \tag{B21}$$

By applying the above consideration to Eq. (B17), one can easily check that this equation satisfies the necessary condition of gauge independence. More importantly, this result shows that the oscillating part of the off-diagonal component can be as important as its time-averaged value. This also implies that by using a time-averaged Floquet master equation, where the oscillations are ignored, some important information about physical quantities could be neglected.

Now, we consider the case of a two-level system. Separating the contribution of diagonal and off-diagonal density matrix components,

$$\overline{\dot\Sigma^{\rm SS}} = -\beta\Big[\overline{\sum_{\alpha\neq\bar\alpha}\langle\phi_{k,\bar\alpha}(t)|\dot\phi_{k,\alpha}(t)\rangle(\epsilon_{k\bar\alpha}-\epsilon_{k\alpha}+i\,\partial_t)\rho^{\rm SS}_{k,\alpha\bar\alpha}} + \sum_\alpha i\,\overline{\dot\rho^{\rm SS}_{k,\alpha\alpha}\langle\phi_{k,\alpha}(t)|\dot\phi_{k,\alpha}(t)\rangle}\Big], \tag{B22}$$

and writing the above in terms of d and u states, we obtain

$$\overline{\dot\Sigma^{\rm SS}} = 2\beta{\rm Re}\big[\overline{\big((\epsilon_{ku}-\epsilon_{kd})\rho^{\rm SS}_{k,du}+i\,\dot\rho^{\rm SS}_{k,du}\big)\langle\dot\phi_{k,u}(t)|\phi_{k,d}(t)\rangle}\big] - \beta\,{\rm Im}\big[\overline{\dot\rho^{\rm SS}_{k,dd}\langle\dot\phi_{k,d}(t)|\phi_{k,d}(t)\rangle}-\overline{\dot\rho^{\rm SS}_{k,dd}\langle\dot\phi_{k,u}(t)|\phi_{k,u}(t)\rangle}\big], \tag{B23}$$

where in the last line we have used that $\dot\rho^{\rm SS}_{k,uu} = -\dot\rho^{\rm SS}_{k,dd}$.

Note that in our simulations $\dot\rho^{\rm SS}_{k,dd}$, which can be read from the Fourier expansions $\rho^{n\rm SS}_{k,dd}$ in Figs. 4 and 5, is almost negligible compared to the off-diagonal component. As a consequence, the main contribution of the entropy-production rate originates from the off-diagonal component of the density matrix. We can also see this at $k = 0$ where exact analytic expressions exist. In particular for weak couplings (as compared to Ω), where the steady-state diagonal density matrix elements have a weak oscillation amplitude, the entropy production can be approximated by

$$\overline{\dot\Sigma^{\rm SS}} \approx 2\beta{\rm Re}\big[\overline{\big((\epsilon_{ku}-\epsilon_{kd})\rho^{\rm SS}_{k,du}+i\,\dot\rho^{\rm SS}_{k,du}\big)\langle\dot\phi_{k,u}(t)|\phi_{k,d}(t)\rangle}\big]. \tag{B24}$$

APPENDIX C: ANALYTIC RESULTS NEAR THE DIRAC POINT ($k = 0$)

In this section, we give some intermediate steps in the derivation of the analytic solutions near the Dirac point. At $k = 0$, the Hamiltonian simplifies to

$$H_{\rm el}(k=0,t) = A_0\begin{pmatrix}0 & e^{i\Omega t}\\ e^{-i\Omega t} & 0\end{pmatrix}, \tag{C1}$$

and exact expressions can be obtained for the Floquet modes [20]. The density matrix at $k = 0$ is (in this appendix we will suppress the k label)

$$W_{\rm el} = \sum_{\alpha\beta}\rho^I_{\alpha\beta}e^{-i(\epsilon_\alpha-\epsilon_\beta)t}|\phi_\alpha(t)\rangle\langle\phi_\beta(t)|. \tag{C2}$$

Note that there are a multiplicity of quasienergy levels, yet there are only two distinct exact eigenstates of the periodic Hamiltonian that we label by "up (u)" and "down (d)" in the main text. The quasimodes $|\phi_{u,d}(t)\rangle$ and the exact eigenstates $|\psi_{u,d}(t)\rangle$ are related as $|\psi_{u,d}(t)\rangle = e^{-i\epsilon_{u,d}t}|\phi_{u,d}(t)\rangle$. As briefly shown in Appendix B, Floquet quasimodes and quasienergies are not uniquely determined. For $k = 0$, the quasienergies may be written as

$$\epsilon_d = m_d\Omega + \frac{-\Omega-\Delta}{2}, \quad \epsilon_u = m_u\Omega + \frac{-\Omega+\Delta}{2}, \tag{C3}$$

where $\Delta = \sqrt{4A_0^2+\Omega^2}$ and $m_{d,u}$ are arbitrary integers. The corresponding quasimodes are then given by

$$|\phi_d(t)\rangle = e^{im_d\Omega t}\begin{pmatrix}d_{1u}\\ e^{-i\Omega t}d_{2u}\end{pmatrix}, \quad |\phi_u(t)\rangle = e^{im_u\Omega t}\begin{pmatrix}d_{1d}\\ e^{-i\Omega t}d_{2d}\end{pmatrix}, \tag{C4}$$

where

$$d_{1u} = \frac{\sqrt{2}A_0}{\sqrt{\Delta(\Delta-\Omega)}}; \quad d_{2u} = \frac{1}{\sqrt{2}}\sqrt{1-\frac{\Omega}{\Delta}}, \tag{C5}$$

$$d_{1d} = \frac{\sqrt{2}A_0}{\sqrt{\Delta(\Delta+\Omega)}}; \quad d_{2d} = -\frac{1}{\sqrt{2}}\sqrt{1+\frac{\Omega}{\Delta}}. \tag{C6}$$

Later we will choose a gauge in which $m_d = m_u = 1$. This results in $\epsilon_u - \epsilon_d = \Delta > \Omega$. The reason for choosing this seemingly unnatural gauge is that as will be clarified later, in this gauge, the transition rates are time independent. However, to avoid the problem of gauge dependence, it is often convenient to construct the matrix elements not between the quasimodes $|\phi_{u,d}(t)\rangle$ themselves as done in the main text, but between the exact eigenstates $|\psi_{u,d}(t)\rangle$. We refer to the matrix elements between the exact eigenstates as the gauge-invariant matrix elements, and the entire Floquet master equation can be written in terms of them. The gauge-invariant matrix elements for our model are $C^{\rm gi}_{1,2\alpha\beta} = C_{1,2\alpha\beta}e^{i(\epsilon_\alpha-\epsilon_\beta)t}$, with the $C_{1,2\alpha\beta}$ being the matrix elements between the quasimodes. We may write

$$C^{\rm gi}_{1\alpha\beta}(t) = e^{i(\epsilon_\alpha-\epsilon_\beta)t}\langle\phi_\alpha(t)|c^\dagger_\uparrow c_\downarrow|\phi_\beta(t)\rangle, \tag{C7}$$

$$C^{\rm gi}_{2\alpha\beta}(t) = e^{i(\epsilon_\alpha-\epsilon_\beta)t}\langle\phi_\alpha(t)|c^\dagger_\downarrow c_\uparrow|\phi_\beta(t)\rangle. \tag{C8}$$

At the Dirac point we find

$$C_{1uu}(t) = \frac{A_0}{\Delta} e^{-i\Omega t}, \tag{C9}$$

$$C_{1dd}(t) = -\frac{A_0}{\Delta} e^{-i\Omega t}, \tag{C10}$$

$$C_{2uu}(t) = \frac{A_0}{\Delta} e^{i\Omega t}, \tag{C11}$$

$$C_{2dd}(t) = -\frac{A_0}{\Delta} e^{i\Omega t}, \tag{C12}$$

$$C^{\rm gi}_{1ud}(t) = -\frac{1}{2}\left(1+\frac{\Omega}{\Delta}\right) e^{-i\Omega t + i\Delta t}, \tag{C13}$$

$$C^{\rm gi}_{1du}(t) = \frac{1}{2}\left(1-\frac{\Omega}{\Delta}\right) e^{-i\Omega t - i\Delta t}, \tag{C14}$$

$$C^{\rm gi}_{2ud}(t) = \frac{1}{2}\left(1-\frac{\Omega}{\Delta}\right) e^{i\Omega t + i\Delta t}, \tag{C15}$$

$$C^{\rm gi}_{2du}(t) = -\frac{1}{2}\left(1+\frac{\Omega}{\Delta}\right) e^{i\Omega t - i\Delta t}. \tag{C16}$$

It is convenient to define the corresponding gauge-invariant rates

$$R^{\rm gi}_{ab,cd} = e^{it(\epsilon_a-\epsilon_b+\epsilon_c-\epsilon_d)} R_{ab,cd}. \tag{C17}$$

The rate equation (18) can be recast in terms of these gauge-invariant rates as follows:

$$\dot{\rho}^I_{k,\alpha\beta}(t) = -\sum_{\delta\gamma}\left[R^{\rm gi}_{\alpha\delta,\delta\gamma}(t)\rho^I_{k,\gamma\beta}(t) + \dots\right], \tag{C18}$$

where $\rho^S_{k,\alpha\beta} = \rho^I_{k,\alpha\beta} e^{-it(\epsilon_\alpha-\epsilon_\beta)}$. In the following, we will solve the Floquet master equation for the density matrix in the Schrödinger picture $\rho^S_{k,\alpha\beta}$.

Now, one can use the freedom in choosing the quasienergy levels and the corresponding quasimodes, such that the rates R become time independent. This is performed by choosing $|\epsilon_\alpha - \epsilon_\beta| = \Delta(1-\delta_{\alpha\beta})$ because only $n_1 = n_2 = \pm 1$ terms survive in Eq. (20). Moreover, in the limit of $A_0/\Omega \ll 1$, where $1-\frac{\Omega}{\Delta} \simeq \frac{2A_0^2}{\Omega^2}$, $1+\frac{\Omega}{\Delta} \simeq 2 + \mathcal{O}(\frac{A_0^2}{\Omega^2})$, we find the following expressions for the rates:

$$R_{uu,uu} = 2\lambda^2\nu\frac{A_0^2}{\Omega^2}(1+2N_0) = R_{dd,dd} = -R_{uu,dd} = -R_{dd,uu}, \tag{C19}$$

$$R_{uu,ud} = -2\lambda^2\nu\frac{A_0}{\Omega}\left[N_- - \frac{A_0^2}{\Omega^2}N_+\right] \simeq -2\lambda^2\nu\frac{A_0}{\Omega}N_-; \quad R_{uu,du} = -2\lambda^2\nu\frac{A_0}{\Omega}(1+N_-), \tag{C20}$$

$$R_{ud,uu} = -2\lambda^2\nu\frac{A_0}{\Omega}\left[N_0 - \frac{A_0^2}{\Omega^2}(1+N_0)\right]; \quad R_{du,uu} = -2\lambda^2\nu\frac{A_0}{\Omega}\left[(1+N_0) - \frac{A_0^2}{\Omega^2}N_0\right] \simeq -2\lambda^2\nu\frac{A_0}{\Omega}(1+N_0), \tag{C21}$$

$$R_{du,ud} = 2\lambda^2\nu N_-; \quad R_{ud,du} = 2\lambda^2\nu(1+N_-); \quad R_{ud,ud} = 2\lambda^2\nu\frac{A_0^2}{\Omega^2}(N_- + N_+), \tag{C22}$$

$$R_{du,du} = -2\lambda^2\nu\frac{A_0^2}{\Omega^2}(2+N_-+N_+); \quad R_{ud,dd} = 2\lambda^2\nu\frac{A_0}{\Omega}\left[N_0 - \frac{A_0^2}{\Omega^2}(1+N_0)\right], \tag{C23}$$

$$R_{dd,du} = 2\lambda^2\nu\frac{A_0}{\Omega}(1+N_-); \quad R_{du,dd} = -2\lambda^2\nu\frac{A_0}{\Omega}\left[\frac{A_0^2}{\Omega^2}N_0 - (1+N_0)\right] \simeq 2\lambda^2\nu\frac{A_0}{\Omega}(1+N_0), \tag{C24}$$

$$R_{dd,ud} = -2\lambda^2\nu\frac{A_0}{\Omega}\left[\frac{A_0^2}{\Omega^2}N_+ - N_-\right] \simeq 2\lambda^2\nu\frac{A_0}{\Omega}N_-. \tag{C25}$$

Above, $N_0 = N(\Omega), N_\pm = N(\Delta \pm \Omega)$.

In general in the steady state, the density matrix can oscillate with frequency Ω. However, for $k = 0$, as one sees above, in this gauge all the scattering rates are constant in time as they do not contain oscillating terms. Therefore, from the discussion of Appendix A, one can deduce that at $k = 0$, the steady-state density matrix attains a constant value $\partial_t \rho^{\rm SS}_{k=0,\alpha\beta} = 0$. Using this in Eq. (18), one finds that the steady-state diagonal and off-diagonal components of the density matrix in the Schrödinger picture are related as follows:

$$\rho^{\rm SS}_{dd} = \frac{R_{ud,du} + {\rm Re}\left[(R_{ud,dd} - R_{du,uu})\rho^{\rm SS}_{du}\right]}{R_{ud,du} + R_{du,ud}}, \tag{C26}$$

$$\begin{aligned} 0 = {} & i(\epsilon_u - \epsilon_d)\rho^{\rm SS}_{du} + (R_{ud,uu} + 2R_{uu,du} - R_{du,uu}) \\ & + \rho^{\rm SS}_{du}(R_{ud,ud} + R_{du,du}) + \rho^{\rm SS}_{du}(2R_{dd,uu} - 2R_{uu,uu} \\ & - R_{ud,du} - R_{du,ud}) + \rho^{\rm SS}_{dd}(2R_{dd,ud} - 2R_{uu,du}). \end{aligned} \tag{C27}$$

The above equations may be used to solve for all the components of the steady-state reduced density matrix. Here, we simply note that at temperatures small as compared to the quasienergy level spacing $|\epsilon_u - \epsilon_d|$,

$$\rho^{\rm SS}_{dd} = 1 + \mathcal{O}\left(\frac{A_0}{\Omega}{\rm Re}\left[\rho^{\rm SS}_{du}\right]\right), \tag{C28}$$

where

$${\rm Re}\left[\rho^{\rm SS}_{du}\right] = \mathcal{O}\left(\frac{\lambda^2\nu}{|\epsilon_d - \epsilon_u|}{\rm Im}\left[\rho^{\rm SS}_{du}\right]\right). \tag{C29}$$

Below we give explicit results only for the imaginary part of the off-diagonal component because as we show below, it is only this component that enters in the steady-state entropy-production rate at $k = 0$. After some algebra, we find that for $A_0/\Omega \ll 1$,

$${\rm Im}\left[\rho^{\rm SS}_{du}\right] \approx -\frac{(\epsilon_u - \epsilon_d)(R_{ud,dd} + R_{du,uu})}{(\epsilon_u - \epsilon_d)^2 + (R_{du,ud} + R_{ud,du})^2}. \tag{C30}$$

By looking at the R-matrix components in the numerator, one can determine the processes which play a significant role in the entropy production. From Eq. (20) for $R^k_{\alpha\beta,\alpha'\beta'}$, the energy conservation requires that the change in the energy of the electrons by $\epsilon_{k\beta'} - \epsilon_{k\alpha'} - n\Omega$ must be supplied by the reservoir. Here, since we have $R_{ud,dd} + R_{du,uu}$ in the numerator, the immediate conclusion is that here we have Floquet-umklapp processes where the initial and final states of the electrons are the same, and correspond to absorbed or emitted phonons with an energy equal to some multiple of the laser frequency. After rewriting Eq. (C30) explicitly in terms of the amplitude and frequency of the drive, we find

$$\mathrm{Im}\big[\rho^{\mathrm{SS}}_{du}\big] = 2\lambda^2_\Omega \nu_\Omega \frac{A_0}{\Omega^2 + (2\lambda^2_- \nu_-)^2(1+2N_-)^2}, \quad \text{(C31)}$$

where the subscripts Ω and $-$ in λ and ν denote the value of these quantities, and hence the reservoir density of states at energy Ω and energy $\Omega_- = \Delta - \Omega \approx 2A_0^2/\Omega$, respectively. Note that Ω_- is the topological gap at the Dirac point.

From above it is clear that at low temperatures compared to the topological gap, so that the Bose function is small, the real part of the off-diagonal density matrix is

$$\mathrm{Re}\big[\rho^{\mathrm{SS}}_{du}\big] = \mathcal{O}\left(\frac{\lambda^4 \nu^2 A_0}{\Omega^3}\right). \quad \text{(C32)}$$

The entropy-production rate as derived in Eq. (B23) for a constant in time steady-state density matrix is

$$\overline{\dot{\Sigma}^{\mathrm{SS}}} = 2\beta(\epsilon_u - \epsilon_d)\mathrm{Re}\big[\overline{\rho^{\mathrm{SS}}_{du}\langle\dot{\phi}_{k,u}(t)|\phi_{k,d}(t)\rangle}\big]. \quad \text{(C33)}$$

From Eq. (C4), one finds

$$\langle\dot{\phi}_{k,u}(t)|\phi_{k,d}(t)\rangle = \frac{-i\Omega A_0}{\Delta}. \quad \text{(C34)}$$

Using the above expressions, we obtain

$$\overline{\dot{\Sigma}^{\mathrm{SS}}} = 2\beta A_0 \Omega\, \mathrm{Im}\big[\rho^{\mathrm{SS}}_{du}\big] \quad \text{(C35)}$$

with $\mathrm{Im}[\rho^{\mathrm{SS}}_{du}]$ given in Eq. (C31).

[1] T. Oka and H. Aoki, Phys. Rev. B **79**, 081406 (2009).
[2] J. I. Inoue and A. Tanaka, Phys. Rev. Lett. **105**, 017401 (2010).
[3] T. Kitagawa, E. Berg, M. Rudner, and E. Demler, Phys. Rev. B **82**, 235114 (2010).
[4] N. H. Lindner, G. Refael, and V. Galitski, Nat. Phys. **7**, 490 (2011).
[5] M. S. Rudner, N. H. Lindner, E. Berg, and M. Levin, Phys. Rev. X **3**, 031005 (2013).
[6] M. Rechtsman, J. Zeuner, Y. Plotnik, Y. Lumer, D. Podolsky, F. Dreisow, S. Nolte, M. Segev, and A. Szameit, Nature (London) **496**, 196 (2013).
[7] M. Hafezi, S. Mittal, J. Fan, A. Migdall, and J. M. Taylor, Nat. Photonics **7**, 1001 (2013).
[8] J. Cayssol, B. Dóra, F. Simon, and R. Moessner, Phys. Status Solidi RRL **7**, 101 (2013).
[9] D. Carpentier, P. Delplace, M. Fruchart, and K. Gawedzki, Phys. Rev. Lett. **114**, 106806 (2015).
[10] G. Jotzu, M. Messer, R. Desbuquois, M. Lebrat, T. Uehlinger, D. Greif, and T. Esslinger, Nature (London) **515**, 237 (2014).
[11] L. D'Alessio and A. Polkovnikov, Ann. Phys. (NY) **333**, 19 (2013).
[12] H. Kim, T. N. Ikeda, and D. A. Huse, Phys. Rev. E **90**, 052105 (2014).
[13] P. Ponte, Z. Papić, F. Huveneers, and D. A. Abanin, Phys. Rev. Lett. **114**, 140401 (2015).
[14] A. Lazarides, A. Das, and R. Moessner, Phys. Rev. Lett. **115**, 030402 (2015).
[15] A. G. Grushin, A. Gómez-León, and T. Neupert, Phys. Rev. Lett. **112**, 156801 (2014).
[16] M. Bukov, S. Gopalakrishnan, M. Knap, and E. Demler, Phys. Rev. Lett. **115**, 205301 (2015).
[17] H. Sambe, Phys. Rev. A **7**, 2203 (1973).
[18] A. Lazarides, A. Das, and R. Moessner, Phys. Rev. Lett. **112**, 150401 (2014).
[19] L. D'Alessio and M. Rigol, Phys. Rev. X **4**, 041048 (2014).
[20] H. Dehghani, T. Oka, and A. Mitra, Phys. Rev. B **90**, 195429 (2014).
[21] H. Dehghani, T. Oka, and A. Mitra, Phys. Rev. B **91**, 155422 (2015).
[22] H. Dehghani and A. Mitra, Phys. Rev. B **92**, 165111 (2015).
[23] Y. Liao and M. S. Foster, Phys. Rev. A **92**, 053620 (2015).
[24] T. Bilitewski and N. R. Cooper, Phys. Rev. A **91**, 063611 (2015).
[25] M. Genske and A. Rosch, Phys. Rev. A **92**, 062108 (2015).
[26] H. Dehghani and A. Mitra, Phys. Rev. B **93**, 205437 (2016).
[27] T. Kitagawa, T. Oka, A. Brataas, L. Fu, and E. Demler, Phys. Rev. B **84**, 235108 (2011).
[28] L. E. F. Foa Torres, P. M. Perez-Piskunow, C. A. Balseiro, and G. Usaj, Phys. Rev. Lett. **113**, 266801 (2014).
[29] A. Kundu, H. A. Fertig, and B. Seradjeh, Phys. Rev. Lett. **113**, 236803 (2014).
[30] A. Farrell and T. Pereg-Barnea, Phys. Rev. B **93**, 045121 (2016).
[31] T. Iadecola, T. Neupert, and C. Chamon, Phys. Rev. B **91**, 235133 (2015).
[32] T. Iadecola and C. Chamon, Phys. Rev. B **91**, 184301 (2015).
[33] K. I. Seetharam, C.-E. Bardyn, N. H. Lindner, M. S. Rudner, and G. Refael, Phys. Rev. X **5**, 041050 (2015).
[34] S. Kohler, J. Lehmann, and P. Hänggi, Phys. Rep. **406**, 379 (2005).
[35] D. W. Hone, R. Ketzmerick, and W. Kohn, Phys. Rev. E **79**, 051129 (2009).
[36] T. Shirai, T. Mori, and S. Miyashita, Phys. Rev. E **91**, 030101 (2015).
[37] Y. H. Wang, H. Steinberg, P. Jarillo-Herrero, and N. Gedik, Science **342**, 453 (2013).
[38] T. Ando, J. Phys. Soc. Jpn. **75**, 124701 (2006).
[39] H. Suzuura and T. Ando, Phys. Rev. B **65**, 235412 (2002).
[40] D. Hsieh, Y. Xia, D. Qian, L. Wray, J. H. Dil, F. Meier, J. Osterwalder, L. Patthey, J. G. Checkelsky, N. P. Ong, A. V. Fedorov, H. Lin, A. Bansil, D. Grauer, Y. S. Hor, R. J. Cava, and M. Z. Hasan, Nature (London) **460**, 1101 (2009).

[41] J. M. Taylor, W. Dür, P. Zoller, A. Yacoby, C. M. Marcus, and M. D. Lukin, Phys. Rev. Lett. **94**, 236803 (2005).

[42] Y. Su, D. Bimberg, A. Knorr, and A. Carmele, Phys. Rev. Lett. **110**, 113604 (2013).

[43] H. P. Breuer and F. Petruccione, *The Theory of Open Quantum Systems* (Oxford University Press, Oxford, UK, 2010).

[44] R. K. P. Zia and B. Schmittmann, J. Stat. Mech.: Theory Exper. (2007) P07012.

[45] S. Deffner and E. Lutz, Phys. Rev. Lett. **107**, 140404 (2011).

[46] C. C. Chicone, *Ordinary Differential Equations with Applications* (Springer, New York, 1999).